BABEŞ–BOLYAI UNIVERSITY

FACULTY OF BIOLOGY AND GEOLOGY

DOCTORAL SCHOOL OF INTEGRATIVE BIOLOGY

PhD THESIS

(SUMMARY)

GENES INVOLVED IN THE SQUALENE-SYNTHASE ACTIVITY AT DIFFERENT CHEMICAL RACES OF *BOTRYOCOCCUS* (CHLOROPHYTA)

PhD Student:

Tiberiu SZÖKE-NAGY

Scientific supervisor:

Prof. univ. Dr. Nicolaie DRAGOȘ

Cluj–Napoca

2019

TABLE OF CONTENTS

Pg.

Key words: *Botryococcus*, biofuel, hydrocarbon, squalene synthase-like, genes, molecular analysis, phylogeny, three-dimensional protein structure prediction.

LIST OF ABBREVIATIONS

aa	Amino acids
DNA	Deoxyribonucleic acid
cDNA	Complementary DNA
ADNg	Genomic DNA
AICB	Algal and Cyanobacterial Culture Collection (AICB) at the Institute of Biological Research, Cluj-Napoca
Ala	Alanine
Arg	Arginine
RNA	Ribonucleic acid
Asn	Asparagine
Asp	Aspartic acid
BLAST	Basic Local Alignment Search Tool
FPP	Farnesyl diphosphate
FPS	Farnesyl pyrophosphate
Gln	Glutamine
Glu	Glutamic acid
GRAVY	Grand average of hydropathy
Leu	Leucine
LG + G	Le Gascuel 2008 model + Gamma distributed
LOS	Lycopaoctaene synthase
Lys	Lysine
ML	Maximum Likelihood
NADPH	Nicotinamide adenine dinucleotide phosphate
NJ	Neighbor-Joining
ONU	United Nations
PCR	Polymerase Chain Reaction
PREFMD	Protein REFinment via Molecular Dynamics
PSPP	Presqualene diphosphate
NMR	Nuclear magnetic resonance
SSL	Squalene synthase-like
SSL-1	Squalene synthase-like 1
SSL-2	Squalene synthase-like 2
SSL-3	Squalene synthase-like 2
TD-PCR	Touchdown PCR
TM	Transmembrane domain
TOE	Tonne of oil equivalent
Tyr	Tyrosine
Val	Valine

INTRODUCTION

The contemporary society will inevitably face a resource crisis, more specifically, the fossil fuel reservoir will be depleted based on the increasing number of Earth's inhabitants (according to UN, there are 7.7 billions inhabitants at the present time and by the end of the 21st century, an impressive number of 12 billion inhabitants is expected), the rising life expectancy and the continual economic growth. The life expectancy has doubled and the energy requirements have increased almost 35 times in the last 2 centuries. Currently, 80% of the globally consumed energy is based on fossil fuels. It is expected that by 2030-2040 the exploitation of natural fossil fuel resources will be at its maximum, closely followed by a steep decline. Undoubtedly, there is a growing need for utilizing renewable energy sources, which can be easily achieved due to the technological advancements in this particular domain.

Microalgae are a source of renewable energy and can be used in biofuel production because of their many advantages, which will be discussed in the Theoretical part of this thesis.

Botryococcus braunii (Class Trebouxiophyceae) is an ideal candidate because it can synthesize high amounts of hydrocarbons which can be up to 86% of their dry weight in optimal growth conditions (Brown *et al*., 1969); these hydrocarbons are similar to those found in fuel reservoirs. Strains of *B. braunii* are classified in four chemical races: A, B, L and S, based on the type of hydrocarbons they synthesize.

The present thesis aimed at: i) morphological characterization, optimization of nucleic acids extraction methods from the microalga biomass and establishing a protocol for the amplification and isolation of the transcripts and the genes involved in the squalene-synthase activity at different strains of *Botryococcus* genus, deposited in the Algae and Cyanobacteria Collection of the Institute of Biological Research, Cluj- Napoca (AICB); 2) identification of the squalene-synthase like primary transcripts and genes and the 3D prediction of the aforementioned proteins structure and domains.

The originality of this thesis is due to the number of investigated algal strains, which were all isolated from regions of Transylvania, and aims to add value to the existing Algae and Cyanobacteria Collection of the Institute of Biological Research, Cluj-Napoca.

I would like to mention that this thesis was written under the close supervision and guidance of my supervisor, Prof. Dr. Nicolae Dragoș, to whom I wish to sincerely thank for the advice given during my PhD years.

Also, I would like to thank to the advisory commission members, Prof. Dr. Corneliu Tarba, Prof. dr. Horia Leonard Banciu, Conf. dr. Vasile Muntean and Conf. dr. Lucian Barbu-Tudoran, for all the help and advice provided, especially for the constructive feedback.

I would like to also thank to acad. prof. dr. Octavian Popescu, CS I dr. Cosmin Sicora, director of the Botanical Garden from Jibou and CS I dr. Cristian Coman for being referents.

I would like to thank to my foreign colleagues from the Institute of Biological Research from Cluj-Napoca, CS III dr. Hegedűs Adriana, CS III dr. Bogdan Drugă, CS III dr. Andreea Baricz and to the technical assistant Dorina Moldovan for their useful advice offered for the experiments in this paper.

Nonetheless, I would like to thank my parents and sister for their love and support given all these years.

Finally, I would like to sincerely thank my friends, PhD student, Sebastian Alin Porav, Mihai Dorin Birtoc, and to my girlfriend, Diana Galea, who supported me and were close to me in my most difficult moments and without whom this paper would not have been finished.

Chapter. I. FOSSIL FUELS GENERAL INFORMATIONS AND SOURCES OF ALTERNATIVE ENERGY

The global consumption of energy is divided as follows, according to figure 1: petroleum remains the main energy source representing 33% of the total used energy, followed closely by coal (27.5%), then natural gas (24.1%), hydroelectricity (6.9%), nuclear power (4.4%), and lastly, the renewable energy comprise a percentage of 4.1% (British Petroleum, 2019). Petroleum is the most important energy source used nowadays, exceeding all the other fuels. Fossil fuels are formed in the ground, at high temperatures and pressure, at comparably low rates in comparison to the high demand and consumption levels. Thus, fossil fuel sources are not considered to be renewable energy sources because there is a significant gap between the formation and consumption of petroleum. For this matter, the future viewpoint is to make a transition towards alternative energy sources and redirect the fast-developing technology in this area (Kirtay, 2009).

The energy sources are classified in two main groups: fossil fuel energy sources and renewable energy sources, which constitute non-renewable and renewable energy resources. Non-renewable resources include coal, petroleum, natural gas and fissile nuclear fuel (uranium and thorium), while renewable power resources include wind, geothermal, solar, hydroelectricity and biomass.

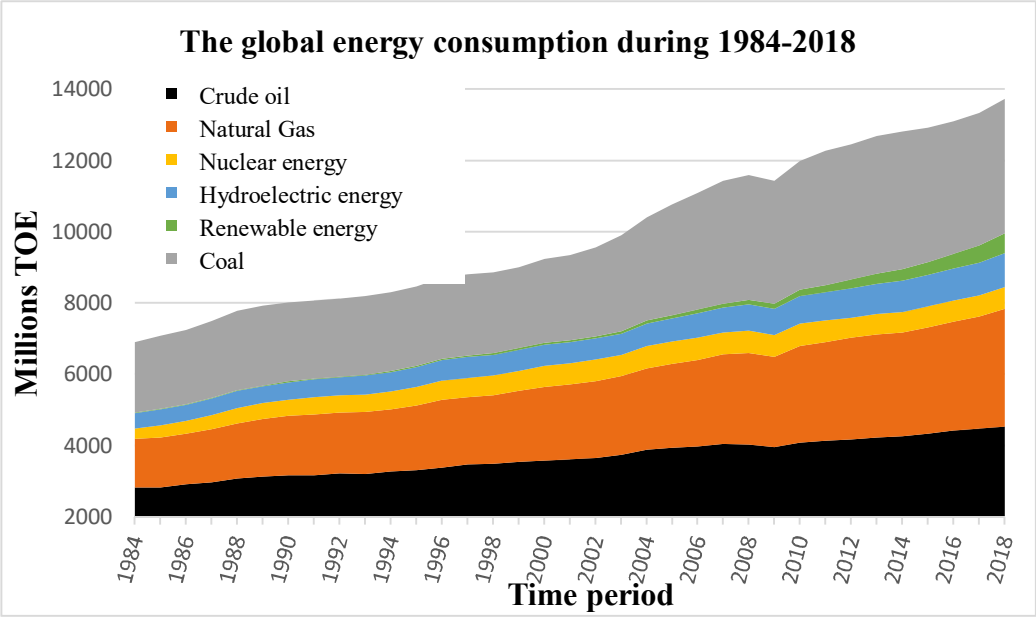

Fig. 1. The global energy consumption during 1984-2018, represented in tonne of oil equivalent (TOE). The global petroleum consumption in 2018 remains the main energy source, with 33% of the total energy consumed (British Petroleum, 2019).

Fossil fuels are currently used to produce over 80% from the total energy, but due to the technological advancements and the new discoveries in the area of renewable energy, there is an interest towards the new renewable energy sources (Demirbas, 2016).

The utilization of fossil fuels as primary sources for energy generation will result in an energy crisis and considerable pollution of the environment. The cost of energy that can be obtained from renewable energy sources (wind, geothermal and solar power, hydroelectricity and biomass) can be competitively attractive with the cost of energy obtained from the non-renewable sources (petroleum, coal and natural gas) because of the advanced technology in this area. As a consequence, the renewable energy sources will become more and more appealing because the fossil resources will become limited (Demirbas, 2016).

The renewable energy sources include: solar energy, hydroelectric energy, wind power, geothermal energy and energy which can be generated from biomass. In 2018, the hydroelectric energy comprised 62.8% of the total utilized alternative energy, followed by wind power (19%), geothermal energy, biomass and other types of alternative energy reaching 9.4%, and the solar energy was used in the lowest amount, with 8.8% (British Petroleum, 2019). Lately, there is an increase in the biofuel production from algae (Dale *et al.*, 2011).

Chapter II. MICROALGAE AND BIOFUELS PRODUCTION – A VIABLE ALTERNATIVE TO FOSSIL FUELS?

Microalgae are photosynthesizing organisms capable of carbon dioxide fixation, from various sources: atmospheric CO_2, CO_2 from industrial processes or dissolved carbonate salts (Brennan and Owende, 2010). The biological CO_2 fixation by microalgae has more advantages because no additional CO_2 is formed and the nutritive compounds are continually consumed, thus hydrocarbons (Judd *et al.*, 2017) or other secondary metabolites of economic interest are produced (da Rosa *et al.*, 2018).

Using microalgae for biofuel production has various advantages: i) microalgae synthesize and accumulate large quantities of neutral lipids (Spolaore *et al.*, 2006; Ghafari *et al.*, 2018); ii) microalgae can be cultivated in areas with favorable climate and be productive the entire year (Chisti, 2007; Demirbas, 2016); iii) microalgae cultivation requires a small quantity of water (Dismukes *et al.*, 2008); iv) microalgae cultivation does not require expensive maintenance treatments (Rodolfi *et al.*, 2008; Ortiz-Marquez *et al.*, 2013); v) algae can have a substantial role in reducing greenhouse gas emissions by capturing CO_2 from different sources (Consoletti and Prinsen, 2019); vi) algae can be used in bioremediation of various pollutants from contaminated wastewater (Cantrell *et al.*, 2008; Salama *et al.*, 2017; Yang *et al.*, 2019); vii) some algal species

can grow in saline or brackish water or coast waters or on non-arable lands, thus not competing with the resources needed in agriculture (Searchinger *et al.*, 2008); viii) the algal biomass can be used to produce biofuels (Voloshin *et al.*, 2016; Bibi *et al.*, 2017).

Biofuels are classified in primary and secondary biofuels. The primary biofuels can be used without additional treatments and the secondary biofuels are used after the biomass has been treated. Secondary biofuels can be further classified into first, second and third generation biofuels, depending on the raw materials they are based on and the treating processes they go through (Nigam and Singh, 2011).

First generation biofuels are formed by fermentation of polysaccharides or starch extracted from culture plants or from corn seeds or other plants with high content of starch (Marzo *et al.*, 2019).

Second generation biofuels are obtained from lignocellulosic biomass. The greatest advantage of these biofuels is the used raw material, which is mainly inedible and thus, does not compete with the food resources (Naik *et al.*, 2010).

Third generation biofuels are derived from bacteria, yeasts or microalgae and consist mainly of bioethanol and biodiesel (Chisti, 2007; Nigam and Singh, 2011).

CHAPTER III. BIOLOGY AND FATTY ACIDS METABOLISM OF *BOTRYOCOCCUS BRAUNII*

Botryococcus braunii (Chlorophyta) is a colonial microalga, that can intracellularly synthesize and then excrete large quantities of hydrocarbons, which are then accumulated in the extracellular colonial matrix. These hydrocarbons are up to 86% of the dry weight of the algal biomass in optimal growth conditions (Brown *et al.*, 1969).

Under the optical microscope, the cells have a pear-shaped form as seen from a lateral position and a rounded shape seen from a vertical position. The cells are most frequently grouped in colonies, but they can be rarely observed singular. The colonies have a spherical, elliptical or even irregular shape (approx. 100 μm), some strains also form sub-colonies which are held together by refringent hydrocarbon string-like connections (Hegedűs *et al.*, 2014). The chloroplast is located adjacent to the plasma membrane, is cup-shaped, has at least 2 major lobes, extending up to the cell apex (Wolf and Cox, 1981). The cells reproduce asexually, by generating 2 to 4 autospores through mitosis (Komárek and Marvan, 1992). The cell also contains mitochondria, endoplasmic reticulum and Golgi apparatus with a high number of vesicles and lipid droplets (Largeau *et al.*, 1980a).

Strains of *B. braunii* synthesize different type of hydrocarbons. *B. braunii* is subclassified in three chemical races: A, B and L. The chemical race A synthesizes n-alkadiene and/or n-trienes and derivatives (C_{23}-C_{33}) (Metzger *et al.*, 1986; Metzger and Largeau, 2005). The chemical race B algae accumulate n-triterpenes, predominantly botryococcenes (C_{30}-C_{37}) (Metzger *et al.*, 1985; Metzger and Largeau, 2005), squalenes and methylated derivatives (Huang and Poulter, 1989; Achitouv *et al.*, 2004). The chemical race L algae synthesize lycopadiene and lycopatriene (Metzger and Casadevall, 1987; Metzger *et al.*, 1990; Thapa *et al.*, 2016). Kawachi *et al*. (2012) have discovered another chemical race of *B. braunii*, named S chemical race, and this algae synthesize n-alkanes and epoxy n-alkanes.

Squalene and botryococcenes synthesis in *B. braunii* consist of two reactions. In the first reaction, two farnesyl diphosphate (FPP) molecules are head-to-head condensed and presqualene diphosphate (PSPP) is formed. In the second reaction, presqualene diphosphate is reduced in presence of NADPH cofactor and squalenes are formed, with a C1-C1' bond between the farnesyl diphosphate molecules (Blagg and *et al.*, 2002). Poulter (1990) suggests that botryococcenes synthesis may take place through a similar mechanism, with the first reaction being common to the squalene synthesis, but in the second part, due to the reduction of PSPP, a C3-C1' bond is formed between the two farnesyl diphosphate molecules. Niehaus *et al*. (2011) use a *de novo* cDNA assembly approach to identify three enzymes involved in the last steps of squalenes and botryococcenes synthesis in *B. braunii*. These enzymes were names squalene synthesis-like. SSL-1 is involved in the condensation of FPP molecules in PSPP, afterwards, PSPP is converted to squalene (SSL-2) or botryococcene, all three reaction are NADPH-dependent.

B. braunii has a great biotechnological potential due to the hydrocarbon synthesis and accumulation in the extracellular matrix. They can be up to 86% of the dry weight, depending on the growth conditions and the strain (Brown *et al.*, 1969; Wolf and Cox, 1981).

The pigments composition of *B. braunii* chemical races was also studied. One of the most important carotenoids found in B and L chemical races is lutein (20-29% of the total carotenoids), followed by β-carotene, echinenone, 3-OH echinenone, canthaxantin, violaxanthin, loroxanthin and neoxanthin (Ranga Rao *et al.*, 2017).

Some *B. braunii* strains produce up to 4.0-4.5 g/L EPS, but they produce few hydrocarbons (5% from the dry weight). Strains belonging to A and B chemical races can produce up to 250 mg/L EPS, while strains belonging to L chemical race produce up to 1g/L (Banerjee *et al.*, 2002).

Chapter IV. OBJECTIVES OF THE STUDY

More than 1300 algal strains from 9 principal phyla (Chlorophyta, Cyanobacteria, Euglenophyta, Xantophyta, Bacillariophyta, Cryptophyta, Rhodophyta, Chrysophyta and Dinophyta) can be found in the Alga and Cyanobacteria Collection of the Institute of Biological Research (AICB) from Cluj-Napoca. Both *B. braunii* race A and *B. terribilis* race B belong to this collection, even if they are not found in impressive numbers, but their importance is of great significance.

Botryococcus braunii is a unicellular, colonial microalga, belonging to Chlorophyta phylum, Trebouxiophyceae class. The importance of this alga comes from its capability to synthesize and accumulate hydrocarbons similar to those found in petroleum deposits. Lately, the synthesis mechanism of these hydrocarbons has been of great interest in the scientific community. However, a mass production of these hydrocarbons cannot be implemented and remains a desired process in the future.

In the present study, the following objectives have been proposed:

- The morphological characterization of *Botryococcus* strains, both race A and race B, found in the AICB Collection, through light and fluorescence microscopy, using Nile Red and Neutral Red dyes.

- Testing nucleic acid extraction methods and standardization of a PCR protocol to amplify and isolate the primary transcripts and the genes involved in the squalene synthase activity.

- Identification of primary transcripts and the SSL genes, analysis of the conserved regions and establishing phylogenetic relationships among enzymes involved in the hydrocarbon synthesis pathways in race B algal strains.

- Three-dimensional protein structure prediction of the main structural domains of squalene synthesis-like proteins, by comparing the proteins found in *B. terribilis* AICB 870 strain and those characterized in *B. braunii* Showa strain.

Chapter V. MATERIAL AND METHODS

V. 1. Algal strains and growth conditions

The algal strains used in this paper were isolated from the algal flora of Transylvania, from various ponds scattered in Cluj, Mureș and Bihor counties. These strains are AICB 53, AICB 413 AICB 414, AICB 415, AICB 416, AICB 438, AICB 442, AICB 475, AICB 870, AICB 872 and AICB 874.

V. 2. Light and fluorescent microscopy

The morphological analysis was made by light and fluorescence microscopy. Nile Red was used to visualize the hydrocarbon content and lipid droplets, whereas Neutral Red was used for visualizing vesicles.

V. 3. Molecular analysis

The protocol established for identifying the primary transcripts and the genes involved in the squalene synthesis activity in *Botryococcus* AICB strains consisted of the following steps: i) growing and obtaining algal biomass (see Section V. 3. 1.); ii) isolation of gDNA and total RNA, by using both commercial kits and the classical phenol:chloroform:isoamyl alcohol extraction method (see detailed information in Sections V. 3.2 and V. 3.3); iii) cDNA synthesis (Section V. 3.4); iv) primer design and *in silico* primer testing, PCR amplification using both standard endpoint PCR and Touchdown PCR, isolation and cloning of the obtained fragments (Section V. 3.5); v) sequencing of the isolated SSL genes, chromatography analysis and contig generation (Section V. 3.6).

V. 4. Phylogenetic analysis

The phylogenetic analysis was made using the available databases, UniProtKB/Swis-Prot and GenBank. Two data sets were used in order to construct phylogenetic trees. One data set contained 68 protein sequences from all groups of organisms that were used for identifying the conserved domains and phylogenetic analysis. The other data set contained 24 proteins from algal organisms that were used for phylogenetic analysis. The sequences were aligned using Mega7 (Kumar *et al.*, 2016), ClustalW algorithm (Larkin *et al.*, 2007) by default settings. The phylogenetic trees were generated using multiple alignments, the following methods: Maximum Likelihood (ML) and Neighbor-Joining (NJ) with a set bootstrap value of 1000 replicates.

V. 5. Three-dimensional protein structure prediction

In order to predict *in silico* the three-dimensional protein structure of SSL, the following steps were carried: i) generation of the raw three-dimensional structure using Phyre2 server (Lawrence *et al.*, 2015); ii) quality control of these structures using the following programs: RAMPAGE (Lovell *et al*., 2003), ProSA-web (Wiederstein and Sippl, 2007) and MolProbity (Chen *et al.*, 2009); iii) structure refinement using GROMACS (Abraham *et al.*, 2015) based on the PREFMD protocol (Heo and Feig, 2018); iv) quality control of the refined structures, using the same programs; v) identifying the functional regions using ConSurf server (Ashkenazy *et al.*, 2016); vi) prediction of the binding sites for ligands using P2Rank (Jendele *et al.*, 2019; Krivák and Hoksza, 2018); and COACH (Yang *et al.*, 2013); vii) visualization of the three-dimensional structures and image generation with UCSF CHIMERA (Peterson *et al.*, 2004).

Chapter VI. RESULTS AND DISCUSSIONS

VI. 1. Light and fluorescence microscopy

The investigated algal strains possess all the morphological characteristics to *B. braunii* race A as described previously by Largeau *et al.* (1980b), Wolf and Cox (1981), Komárek and Marvan (1992), Weiss *et al.* (2012), Hirose *et al.* (2013), Hegedűs *et al.* (2016).

The colonies are loose, have a spherical (Fig. 2-D1) or elliptical shape. The dimension of the colonies varies between 21 µm (Hegedűs *et al.*, 2016) and 80 µm (Fig. 2-D2). The extracellular matrix is composed of a crosslinked hydrocarbon network (Fig. 2-D2). The cells are bound by a cup-shaped mucilaginous (Fig. 2-A2), telescopic and stratified (Fig. 2-C1), hydrocarbon rich (Fig. 2-B2, Fig. 2-C2) sheath. The sheath covers almost 2/3 of the cell, with the exception of the apical region, which forms a colorless polysaccharides cap (Fig. 2-A4), without any hydrocarbons (Fig. 2-B4).

The double-dyed technique (Nile Red and Neutral Red) revealed the presence of vesicles and the lipid droplets, which are closely related to the algal growth phase and cellular division (Fig. 2 A1-3).

The morphological observations of *Botryococcus* AICB 413, 414, 418, 438, 442 and 870 algal strains (Fig. 3) showed a pear (Fig. 3D) or spherical (Fig. 3-E1) shape of the algal colonies.

The sub-colonies are compact, held together by mucilaginous string-like connections (Fig. 2-3A, C, D-black arrow), rich in hydrocarbons (Fig. 3B – white arrow). In some cases, AICB 870 strain possessed at the periphery side of the colonies short, irregular, mucilaginous processes, sometimes they can appear branched (Fig. 3A, C, D – white arrow); these mucilaginous processes are rich in hydrocarbons (Fig. 3B). In some cases, hydrocarbon droplets could be observed on these string-like connections or nearby colonies (Fig. 3E1).

The cells are pear-shaped and are defined by a cup-shaped mucilaginous sheath, radially directed, and partially or totally embedded in a hydrocarbon rich mucilaginous matrix (Fig. 3B and E3).

The lipid droplets were observed under the fluorescent microscope using Nile Red dye (Fig. 3B, E3); these droplets are abundant and have variable dimensions. They play an important role in the extracellular excretion of hydrocarbons and their accumulation in the extracellular matrix. In some cases, hydrocarbon droplets can be observed because of the lamellar pressure (Fig. 3 E1).

All the observations made by light microscopy indicate that the investigated *Botryococcus* AICB strains have all the characteristics specific to *B. terribilis*, according to the descriptions made by Komárek and Marvan (1992), Treviño *et al.* (2009), Mendes *et al.* (2012), Hegedűs *et al.* (2014).

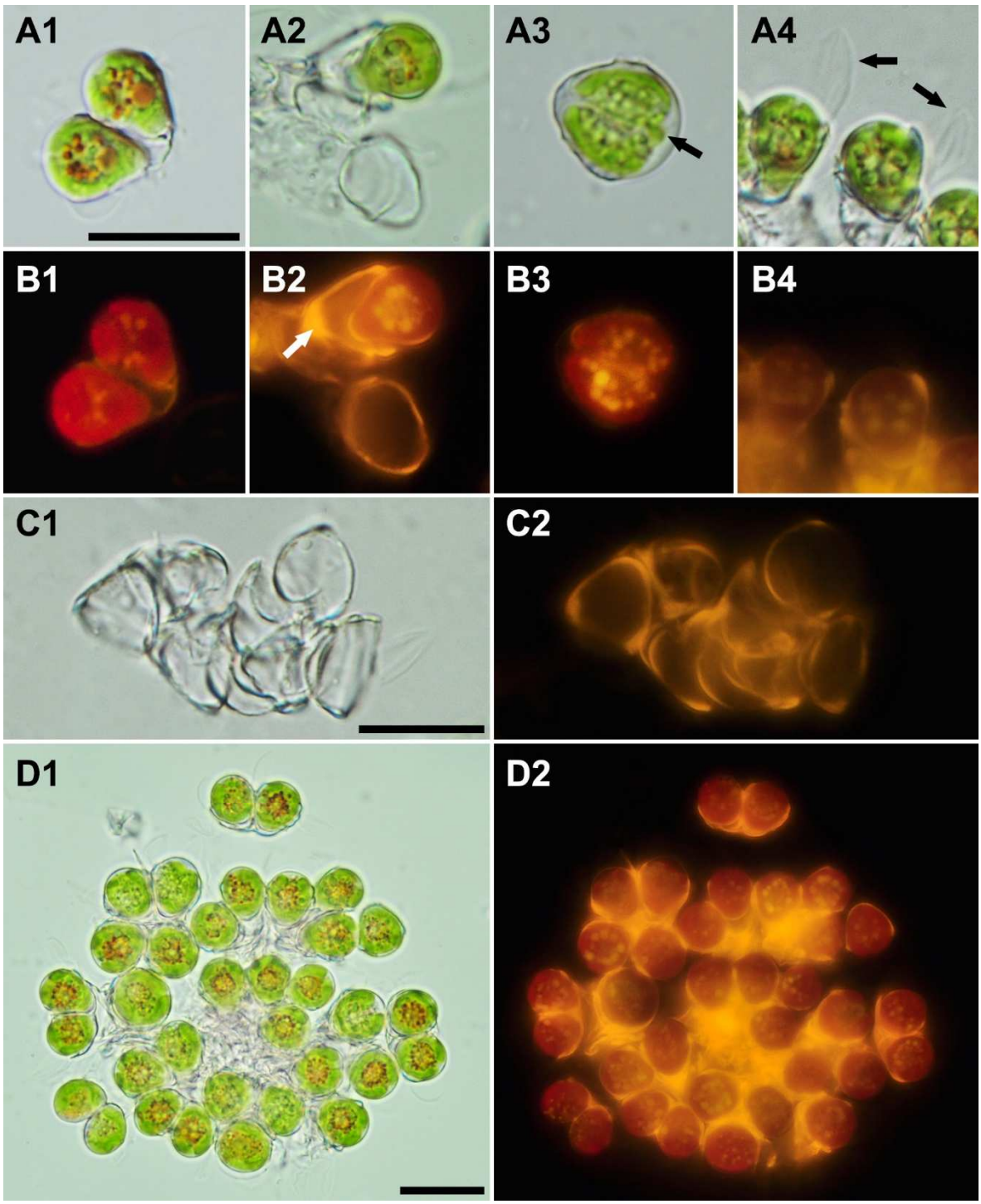

Fig. 2. Light and double-dyed fluorescence microscopy (Nile Red and Neutral Red) on algal cells of *B. braunii* AICB 53. The cells are found in different division phases: cells in interphase have a large number of red, neutral-positive, centrally-located vesicles (A1) and few lipid droplets (B1); cells already in division or that enter mitosis have a few vesicles (A2) and an increasing number of lipid droplets (B2); once the septum is formed, the number and volume of the lipid droplets is increasing (B3). The cells have at the apical pole a polysaccharide (B4) cap (A4), and are surrounded by a hydrocarbon rich (C2) cup (B2, C1). The cell form loose colonies (D1), which are embedded in a hydrocarbon rich extracellular matrix (D2). The images have Nomarski effect. Bar = 20 µm for all images.

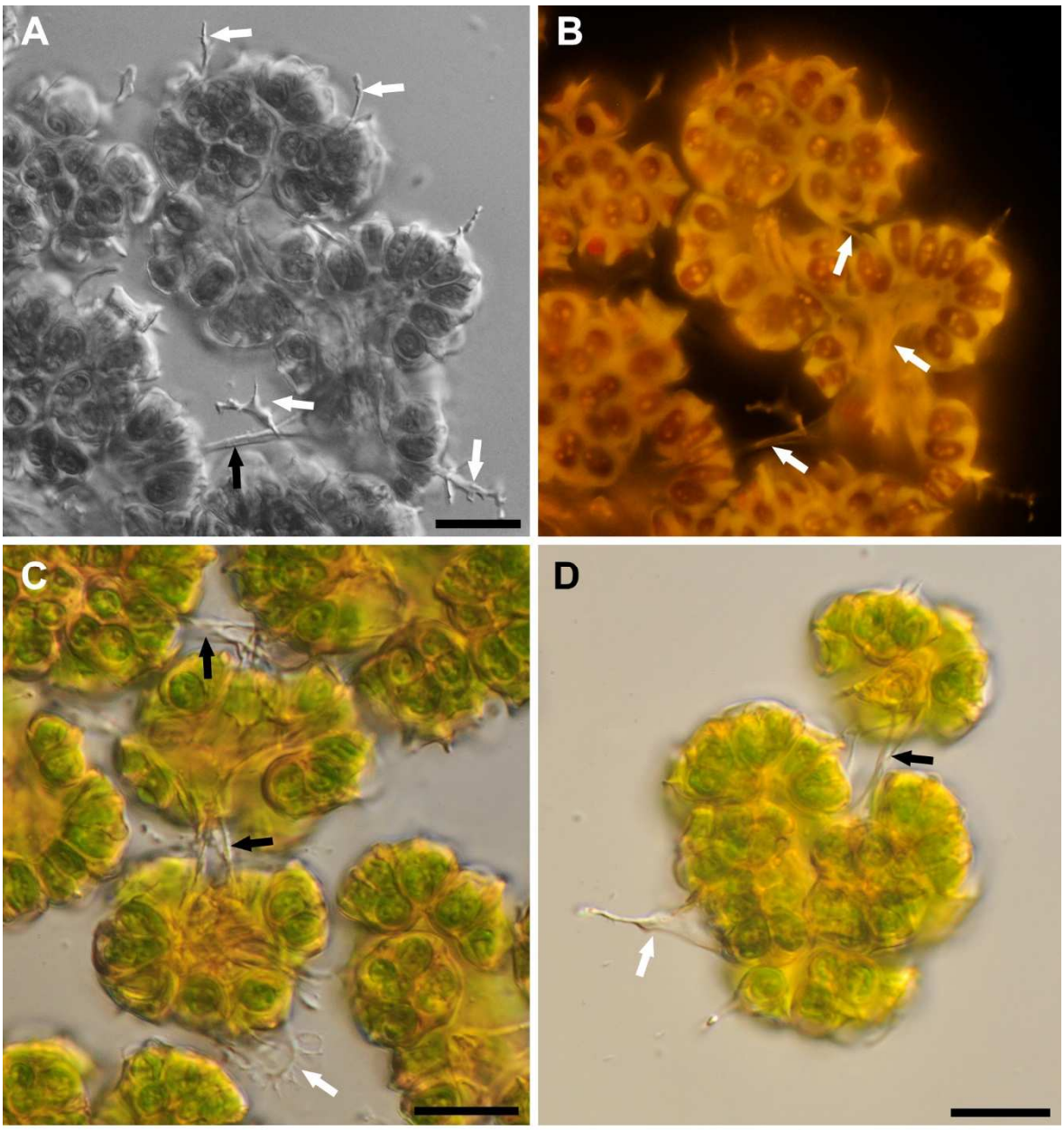

Fig. 3. Light microscopy images that show the colonial organization of *B. terribilis* AICB 870 (A-D). The sub-colonies are held together by mucilaginous string-like connections (A, C, D – black arrow) and various mucilaginous processes (A, C, D – white arrow) that are impregnated with hydrocarbons (B).

VI. 2. Molecular analysis

VI. 2. 1. DNA and RNA isolation

Nucleic acids were isolated using various commercial kits and also with the phenol-chloroform-isoamyl alcohol (PCI) method. The obtained nucleic acids yields highlighted the following conclusions: ZR Soil Microprobe DNA MiniPrep^{TM} and the PCI extraction method gave the best results, with high yield and purity of nucleic acids. The highest yield of DNA was obtained from AICB 416 strain (398.9 ng μL^{-1}, with a value of 2.16 at A_{260}/A_{280} ratio and 2.30 at A_{260}/A_{230}

ratio). The highest yield of RNA was obtained from AICB 874 strain (3228.4 ng μL^{-1}, with a value of 1.98 at A_{260}/A_{280} ratio and 1.92 at A_{260}/A_{230} ratio). The obtained data are comparable with the data obtained by Kim *et al.* (2012) and Ghawana *et al.* (2011), where similar isolation methods were used for various *B. braunii* strains.

VI. 2. 2. PCR amplification of primary transcripts of SSl-1, SSL-2 and SSL-3 genes

The squalene synthase-like primary transcripts from chemical race B (Fig. 4) were amplified by TD-PCR, by screening between a large set of primer combinations. The amplified PCR products with the *de novo* designed primers were checked on agarose gel electrophoresis.

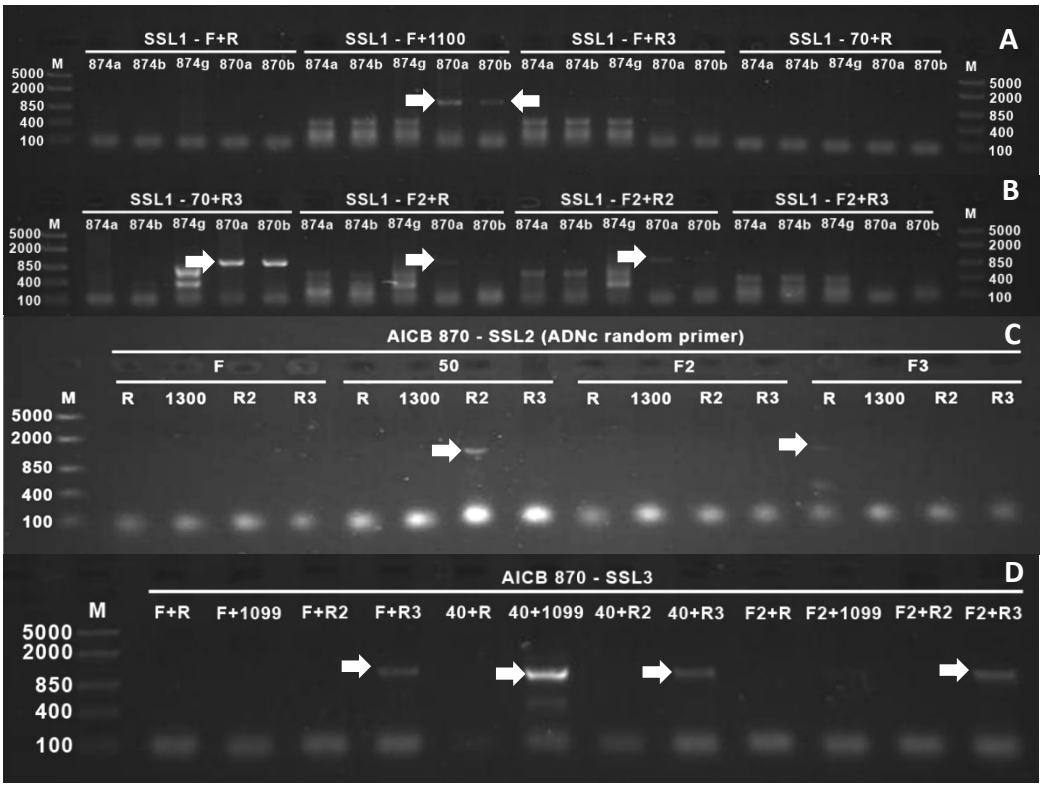

Fig. 4. Agarose gel electrophoresis of the primary transcripts for SSL-1 (A and B), SSL-2 (C) and SSL-3 (D) obtained by TD-PCR. (A-B) TD-PCR using as template cDNA synthesized with universal primers (870a, 874a), oligo $(dT)_{18}$ (870b, 874b) or gDNA (874g). The amplified fragments that represent the three primary transcripts are indicated with a white arrow.

VI. 2. 3. PCR amplification of SSL-1, SSL-2 and SSl-3 genes

SSL genes were amplified by gradient PCR (the thermal gradient was applied during primer annealing), which resulted in the successful amplification of the SSL-1 gene (Fig. 5A), a single 4000bp DNA fragment, and 4 different DNA fragments, varying between 400-2000bp length, that were thought to belong to SSL-3 gene. However, for the downstream applications only the 2000bp DNA fragment was chosen (Fig. 5B). The DNA fragments were gel isolated and cloned before being

sent to sequencing. The genes belonging to the chemical race B strains could not be amplified and isolated from strains belonging to chemical race A.

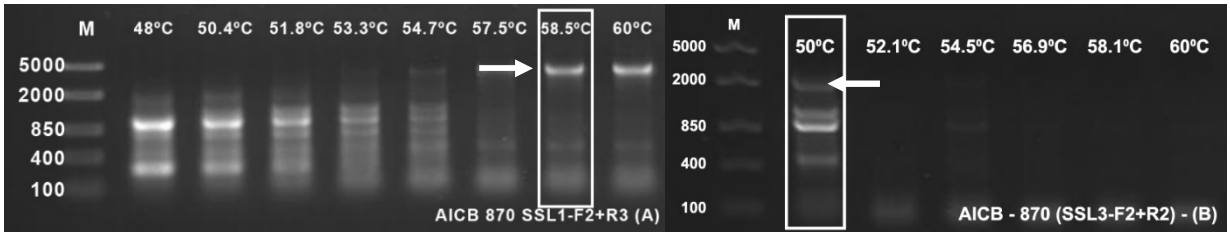

Fig. 5. Agarose gel electrophoresis of PCR products obtained after amplification of SSl-1 (A) and SSL-3 (B). The framed samples were selected for subsequent analysis.

SSL-1 gene was amplified in chemical race B strains with SSL1-F2 and SSL1-R3 primer pair. Agarose gel electrophoresis highlighted the presence of amplified DNA products in the following strains: AICB 413, 414, 416, 438, 442 and 872. The length of the amplified DNA products was similar to that of AICB 870 strain.

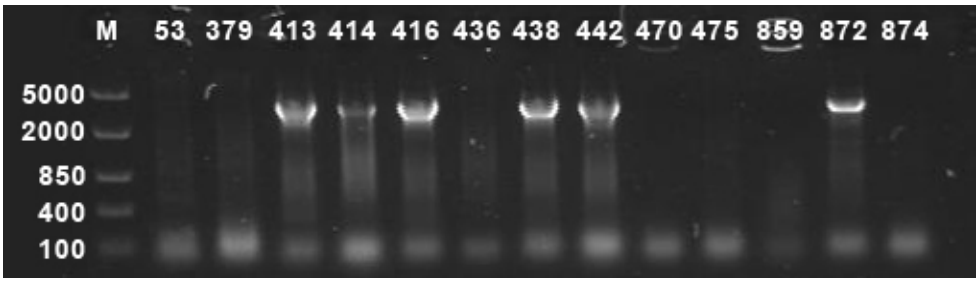

Fig. 6. Agarose gel electrophoresis of amplified SSL-1 gene from the following AICB strains: 413, 414, 416, 438, 442 and 872.

VI. 2. 4. Sequencing and identification of squalene-synthase like genes

The obtained DNA chromatograms after sequencing were manually annotated and compared using BLAST algorithm. The DNA fragments amplified and isolated in this study showed a 95.78% to 99.91% identity to *Botryococcus braunii* Showa genes (HQ585058.1, HQ585059.1 şi HQ585060.1), published by Niehaus *et al.* (2011) according to the BLAST report.

The DNA fragments were sequenced by the primer walking technique because of their high length. The following contigs were generated after assembly and annotation: AICB 413 (3828pb), AICB 414 (3615pb), AICB 416 (3845pb), AICB 438 (3614pb), AICB 442 (3755pb), AICB 870 (3821pb) and AICB 872 (3811pb).

SSL-1 gene structure was determined based on alignments between the nucleotide sequences and the primary transcripts fragments. SSL-1 gene isolated from AICB strains has 8 exons, varying

in length between 101 and 246 nucleotides, and 7 introns varying between 345 and 675 nucleotides. Chromatogram analysis (Fig. 7) also revealed the 864-940 repeated sequence of intron 2. Repeated sequences or GC-rich sequences are characteristic of eukaryotic gene organization (Amit *et al.*, 2012). These regions can be sequenced with great difficulty due to secondary structures formed by the DNA template and the need for a higher melting temperature in order to be denatured (Choi *et al*, 1999).

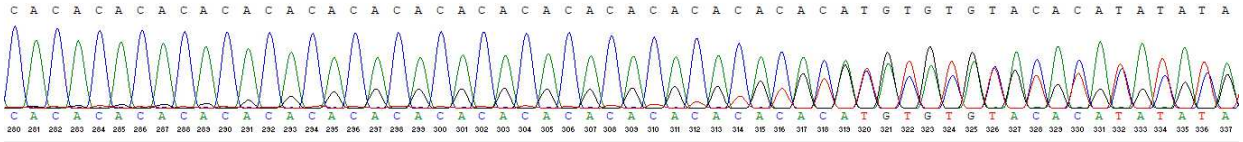

Fig. 7. Chromatogram of a DNA fragment, that indicates the repetitive region 864-940 obtained after SSL-1 gene sequencing (AICB 870) with SSL1-G2F primer.

VI. 2. 5. Analysis of the conserved domains

The multiple alignment between the investigated squalene synthase-like proteins and those found in databases showed 4 conserved domains, 2 aspartate-rich motifs that bind divalent Mg^{2+} ions and a NADPH binding motif. These domains and motifs were also previously described by Nakashima *et al.* (1995), Hata *et al.* (1997), Gu *et al.* (1998) and Lee and Poulter (2008). In this paper, the domains were numbered I-IV and are similar to those described by Lee and Poulter (2008).

VI. 2. 6. Phylogenetic analysis

The phylogenetic trees showed common features of squalene synthase proteins, irrespective of the used algorithm, ML or NJ. The generated phylogenetic trees were grouped in 3 principal clades (Fig. 8): I clade (Tracheophyta), II clade (*Botryococcus*) and III clade (phyla Chordata, Ascomycota and Basidiomycota).

SSL protein sequences belonging to II clade were grouped in 3 distinct sub-clades: subclade II.1 was comprised of SSL-1 (100/100), subclade II.2 was comprised of SSL-2 and LOS sequence (99/93), subclade II.3 was comprised of SSL-3 and a sequence of Songkla Nakarin chemical race L strain (36/47).

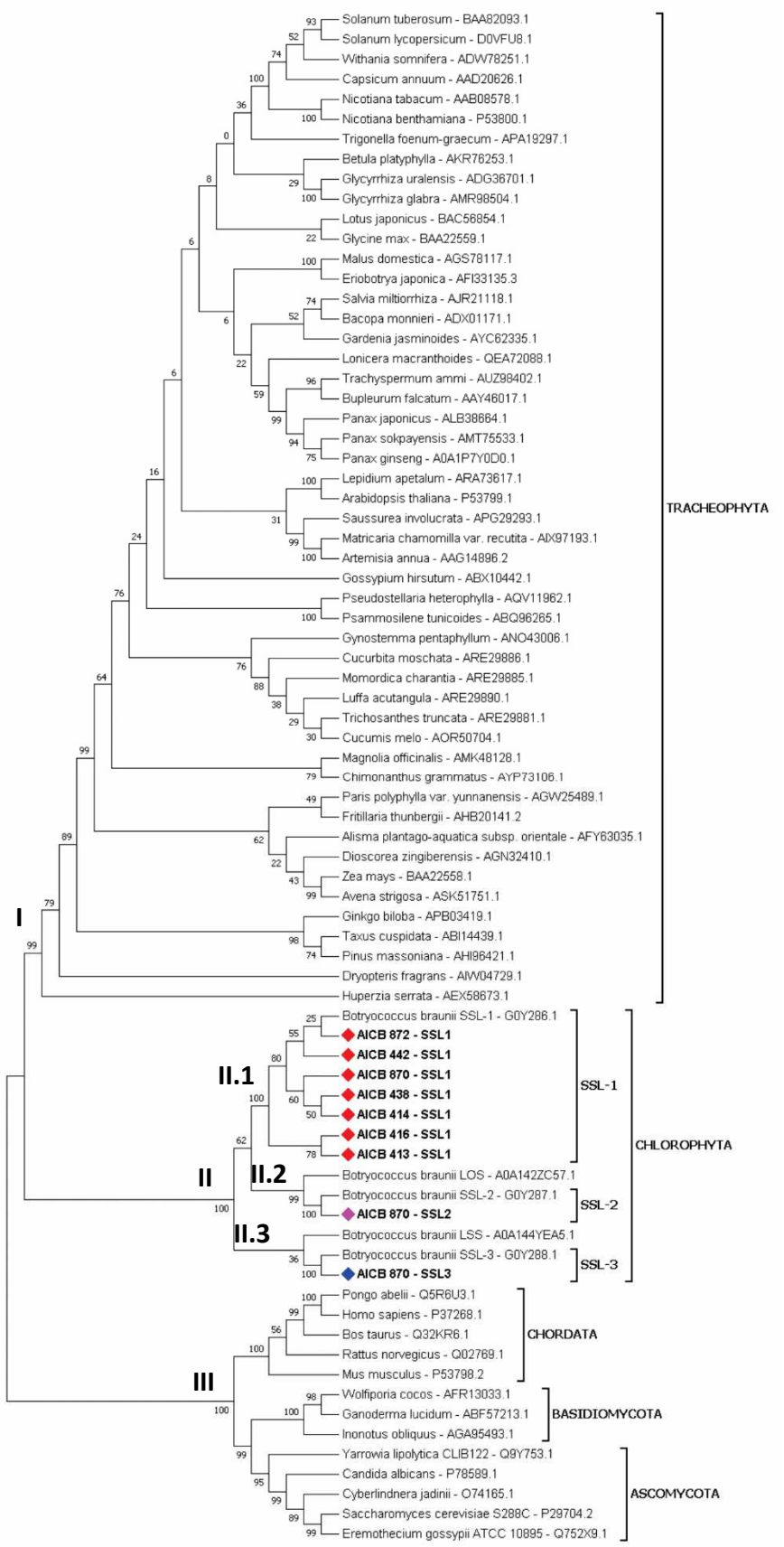

Fig. 8. Phylogenetic tree of squalene-synthase sequences from AICB strains and databases, built by ML algorithm, LG+G model. The branch numbers indicate the bootstrap value, from 1000 replicates.

VI.3. Three-dimensional protein structure prediction

VI. 3. 1. Primary structure analysis (physico-chemical parameters)

The analyzed physical and chemical parameters were: i) amino acid sequence length (aa); ii) molecular weight; iii) theoretical isoelectric point (pI); iv) total number of negatively charged residues (Asp + Glu); v) total number of positively charged residues (Arg + Lys); vi) total number of atoms; vii) extinction coefficient; viii) estimated half-time; ix) instability index and x) GRAVY index. The physical and chemical parameters were computed using the ProtParam tool of ExPASy (Gasteiger *et al.*, 2005).

The physical and chemical parameters analysis revealed similar values for most of the parameters, however, the different values resulted from the partial sequences of SSL-2 and SSL-3. SSL-1 had a unique pI value, 7.96, and also a positive electrical charge in comparison to the neutrally charged SSL proteins from *B. braunii*.

VI. 3. 2. Secondary structure analysis

All three SSL proteins have approximately the same number of α-helix and β-sheet motifs, according to the secondary structure prediction. However, the AICB 870 SSL-2 protein has only 2 TM domains and the Showa SSL-2 protein has 3 TM domains. The 2 transmembrane domains found in AICB 870 SSL-2 protein are represented by the CHYVAGLVGCAVAKIF *aa* sequence between 136-151 and RLLLVVGVVAYFVYAFN *aa* sequence between 364-379. The N- and C-terminus are found on the same membrane side due to the partial sequence of SSL-2. The *B. braunii* Showa SSL-2 protein has the following TM *aa* sequences: CHYVAGLVGSAV between 169-184, RLLLLVGVVAYFAYAF between 397-412 and KGLAVASVALLLLVLLA between 435-351. A model of the generated report with Phyre2 of to the secondary structure prediction of *B. terribilis* AICB 870 SSL-2 protein is illustrated in Fig. 9.

VI. 3. 3. Three-dimensional structure prediction

The three-dimensional protein structures of *B. terribilis* AICB 870 and *B. braunii* Showa (available in GenBank) squalene synthase-like proteins were generated using Phyre2 server. The structure prediction was generated by homology analysis with proteins whose structures were experimentally obtained, by RMN or X ray methods. The models used for structure prediction were: 3wcc_C (*Trypanosoma cruzi* squalene synthase*)* and lezf_A (human squalene synthase), the N and C-terminus of proteins were *ab initio* constructed, due to lack of information regarding the end terminus amino acid sequences.

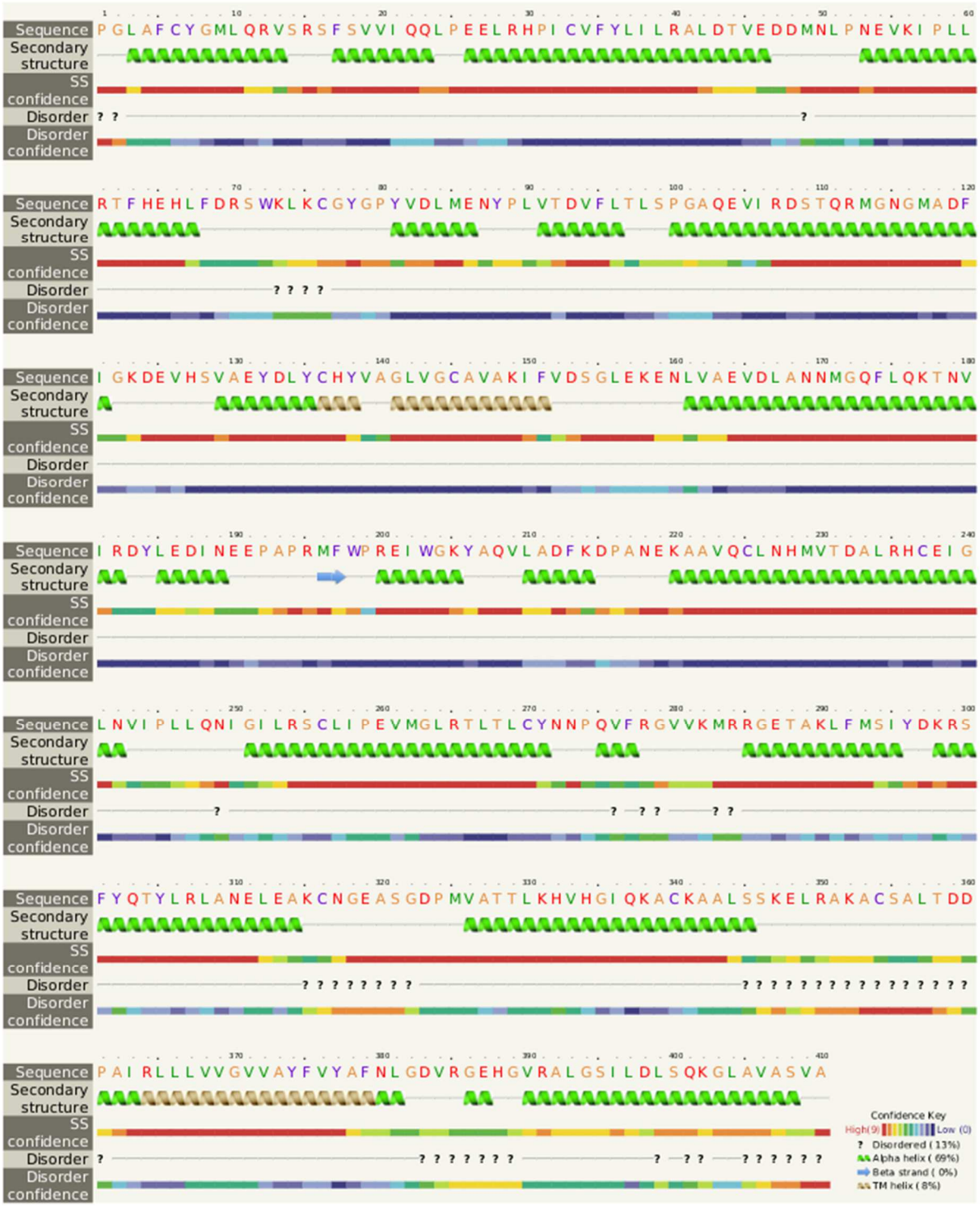

Fig. 9. Secondary structures (α-helix and β-sheet) of squalene synthase-like 2 from *B. terribilis* AICB 870 predicted with Phyre2. According to the predicted secondary structures, SSL-2 has: 13% disordered regions, 69% α-helix, a single β-sheet and 8% TM α-helix.

339 amino acids were modelled with more than 90% confidence for SSL-1 (*B. terribilis* AICB 870) after comparing the aforementioned models. These amino acids represent 85% of the protein structure, meanwhile the rest of the structure, the remaining end regions, were *ab initio* modelled due to lack of structural homology.

In the case of SSL-2 (*B. terribilis* AICB 870), although the overall identity was higher, the percentage of high confidence modelled residues was lower. This domain is formed of 334 amino acids and is located in the central part of the protein, representing 83% of the protein total structure. The *ab initio* modelled residues showed a lower confidence than 90% and were predominantly found in the distal regions of the proteins, forming their ends.

SSL-3 structural model (*B. terribilis* AICB 870) was predicted with the highest confidence score from all three proteins analyzed in AICB 870 strain. A 319 amino acid structural fragment was predicted with >90% confidence. This domain constitutes 91% of the protein structure and forms the core part of the protein. The end parts of the protein could not be predicted based on models and were modelled *ab initio*. Squalene synthase-like proteins from *B. braunii* Showa were predicted in a similar way.

The generated three-dimensional protein structures were qualitatively assessed by three distinct methods: ProSA-web, Ramachandran plots (RAMPAGE) and a qualitative global evaluation (MolProbity).

ProSA-web quality assessment indicated high-quality, promising results (Fig. 10). On the other hand, Ramachandran plot indicated that not all generated models are qualitative enough. For SSL-1 AICB 870 (Fig. 11 A_1), only 86.5% of the amino acids were classified in favored regions, while 15 amino acids remained in unallowed regions. A similar result was obtained for the structural model of SSL-2 AICB 870 (Fig. 11 B_1). 86.3% of amino acids were found in favored regions, while 20 residues were located in unallowed regions.

An additional quality test was used due to the inconsistency of the other two analysis. This quality test is a structure-validation service based on experimentally obtained protein structures. All predicted models were subjected to MolProbity validation program, which adds the hydrogen atoms and provides detailed all-atom contact analysis. Quality structure evaluation depended only on the global score of the protein, without local validation between carbon atoms from α and β positions. Based on this analysis, only SSL-3 AICB 870 tridimensional model was similar enough to a native structure with a global score of 3.05 (MolProbity score), followed by SSL-1 AICB 870 with 3.84 and SSL-2 AICB 870 with 3.93.

The previously predicted protein structures were subjected to a refinement process, by applying the protocol used by PREFMD program, which refines the predicted structures by molecular dynamics simulation. The protocol is described in section VI. 3. 3. 2.

The overall structure of the predicted proteins was improved after refinement. In the case of SSL-1 protein from *B. terribilis* AICB 870, the percentage of amino acids found in the favored region rose from 86,5% to 96,3% (Fig. 11 A_2), and the number of residues from unallowed regions was reduced (Tyr119, Asn195, Arg234, Lys 356 and Gln357). This result was confirmed by the

global score obtained with MolProbity which was also reduced from 3.84 to 1.17. ProSA-web analysis (Fig. 10 A_2) indicated a minor change of the Z score. SSL-2 AICB 870 protein structure was also qualitatively improved, the percentage of residues located in the favored region rose to 94,4% and the number of residues in the unallowed region dropped to 4 residues: Pro225, Arg228, Lys315 and Asp330 (Fig. 11 B_2). The global score based on MolProbity validation improved from 3.93 to 1.26. SSL-3 protein showed a qualitative improvement after the refinement process, by which the percentage of residues located in the favored region rose with 2% and reached 97.7%, while the residues located in the unallowed regions remained the same (Fig. 11 C_2). The Z score obtained with ProSA-web was slightly improved from -7.30 to -6.47 for SSL-2 (AICB 870) (Fig. 10 B_2), but for SSL-3 (AICB 870) the Z score remained the same (Fig. 10 C_2).

The core part of the protein is almost identical between predicted and refined models according to a comparative analysis between the raw and refined structures. The α helix motifs that form the protein core were found to be stable, due to a high degree of symmetry and superimposition between models (Fig. 12). Minor modifications could be noticed at the loop structures, which was expected due to the high flexibility of these secondary structures.

In the case of SSL-1 (AICB 870), a disordered fragment could be noticed (Fig. 12 A1), formed by 14 amino acids, which during refinement suffered a conformational change by 90° at Lys40 and Asp41 (Fig. 12 A2). The same process was observed at the C-terminus where the chain suffered a conformational change at Lys385.

In the case of SSL-2 (AICB 870), the structure has an anchor which includes one of the transmembrane domains (Fig. 12 B1 and B2). This structural difference results from the conformational change of Lys344 towards Ala343 by 30°.

After the refinement of SSL-3 (AICB 870) (Fig. 12 C1), two minor conformational changes appeared. These changes came from 2 twists present in the only region with intrinsic disorder. The first twist was identified between Arg28 and Lys29, and the second twist appeared towards Asp32 and was identified at Glu32.

SSL-3 tridimensional model (Fig. 12 C1) showed the smallest conformational change after refinement from all three squalene synthase-like proteins from AICB 870, because the raw model was initially of great quality. One of the reasons which lead to such a qualitative model was the lack of disordered regions in comparison with SSL-1 and SLL-2. The disordered regions still constitute one of the main reasons why 3D structure prediction is both computationally and experimentally difficult to achieve, these disordered regions have high instability and flexibility.

After superimposing the squalene synthase-like pairs (SSL-1 Showa - SSL-1 AICB 870; SSL-2 Showa - SSL-2 AICB 870; SSL-3 Showa - SSL-3 AICB 870), some differences were observed at the end N- and C-terminus regions of the polypeptide chains. However, the local

analysis of these regions indicated the presence of structural homology between them and the differences reside from a symmetrical change of these regions. This is a common feature among regions with intrinsic structural variability and high disorder. This summary presents the comparison after superimposing 3D structures belonging to SLL-1 from Showa and AICB 870.

Squalene synthase-like from Showa and AICB 870

The amino acid sequence alignments of SSL-1 showed 5 mismatches at residues from the following positions: 24, 124, 256, 259 and 263. The first two mismatches did not influence neither the secondary, nor the tertiary structure (Fig. 13) because they were situated in a good structured α-helix. The only visible difference was found at position 256 due to a loop formation. At this position, Glu256 (Showa) was replaced by Lys256 (AICB 870) and it lead to a more pronounced bend of the loop. Although there were no significant structural differences between the two SSL-1 proteins, there was a significant difference of the isoelectric point. In the case of SSL-1 (Showa) the pI was 7.12 and the SSL-1 (AICB 870) pI was 7.96. This significant change in the isoelectric point could be explained due to the substitution of Asp256, a negatively charged amino acid, with Lys256, a positively charged amino acid, and the presence of Arg263.

The prediction of active and ligand-binding sites was generated using P2Rank (*et al*., 2019; Krivák and Hoksza, 2018) and the conservation degree was verified using ConSurf (Ashkenazy *et al.*, 2016).

All analyzed structures presented two potential ligands: FPS – farnesyl phyrophosphate and PS7{(1R,2R,3R)-2-[(3E)-4,8-dimethylnona-3,7-dien-1-yl]-2-methyl-3-[(1E,5E)-2,6,10-trimethylundeca-1,5,9-trien-1-yl]cyclopropyl}methyl trihydrogen diphosphate. Mg^{2+} divalent ions were also identified that could be possibly involved in securing ligand binding to the active site.

Pocket prediction at SSL-1 AICB 870 indicated the presence of four potential pockets, but only one of them was considered due to the high confidence score (Fig. 13 A1). SSL-2 from *B. terribilis* AICB 870 showed nine potential pockets, but only the first one presented a score >50 and the others were eliminated (Fig. 13 C1). Similarly, pocket prediction in the case of *B. braunii* Showa indicated the same pocket number as in the case of all interrogated SSL proteins.

The identified pockets were partially superimposed with the four conserved domains that were analyzed in section VI. 2. 5. Moreover, the amino acids involved in pocket formation indicated a high conservation degree. These observation lead to the conclusion that the head-to-head condensation of FPP moieties takes place in these pockets, which resulted in PSPP formation (SSL-1), followed by conversion to squalene (SLL-2) or botryococcene (SSL-3).

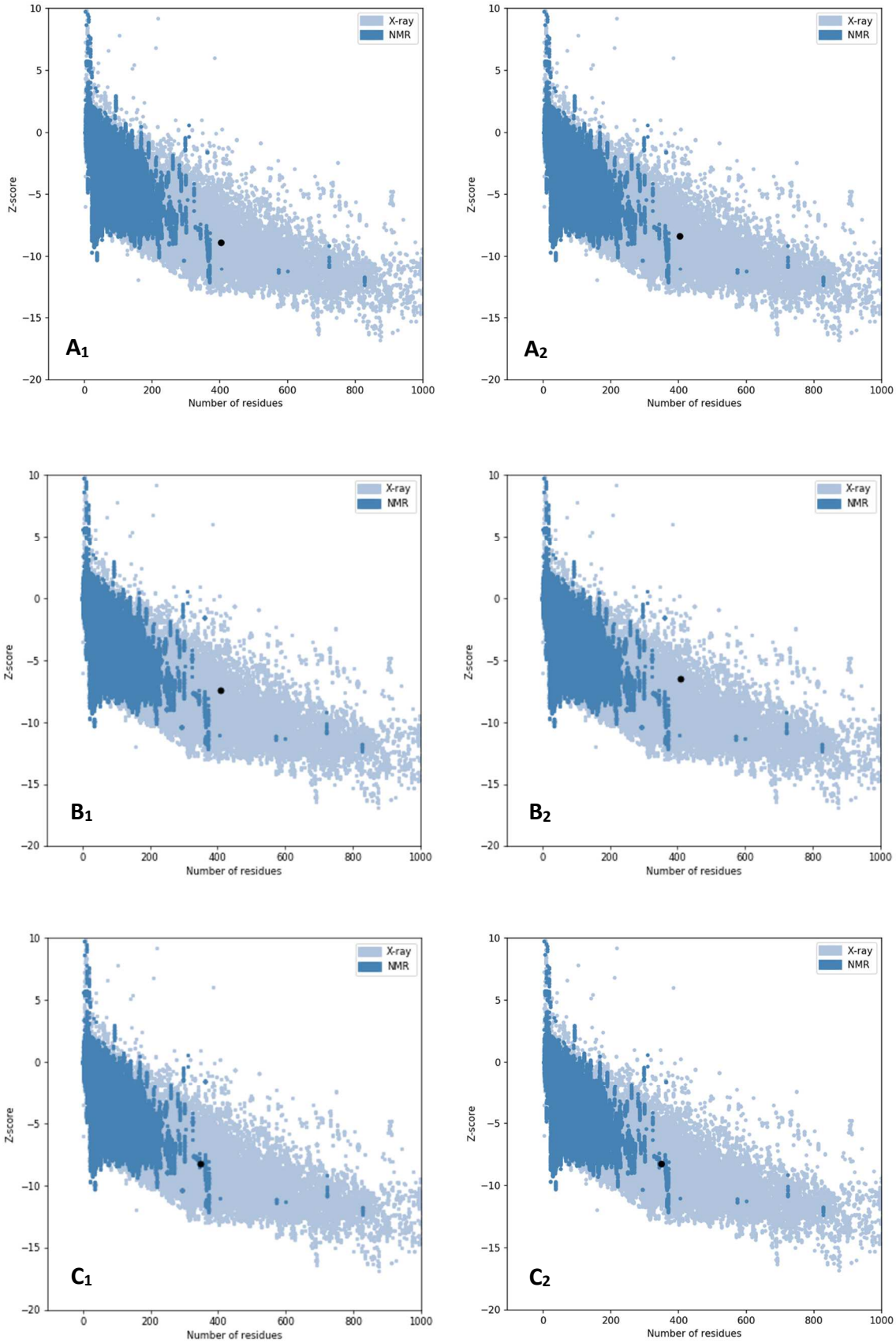

Fig. 10. Schematic representation of the obtained Z score with ProSA-web of SSL-1 (A), SSL-2 (B) and SSL-3 (C) from *B. terribilis* AICB 870, before (subscript 1) and after (subscript 2) structure refinement.

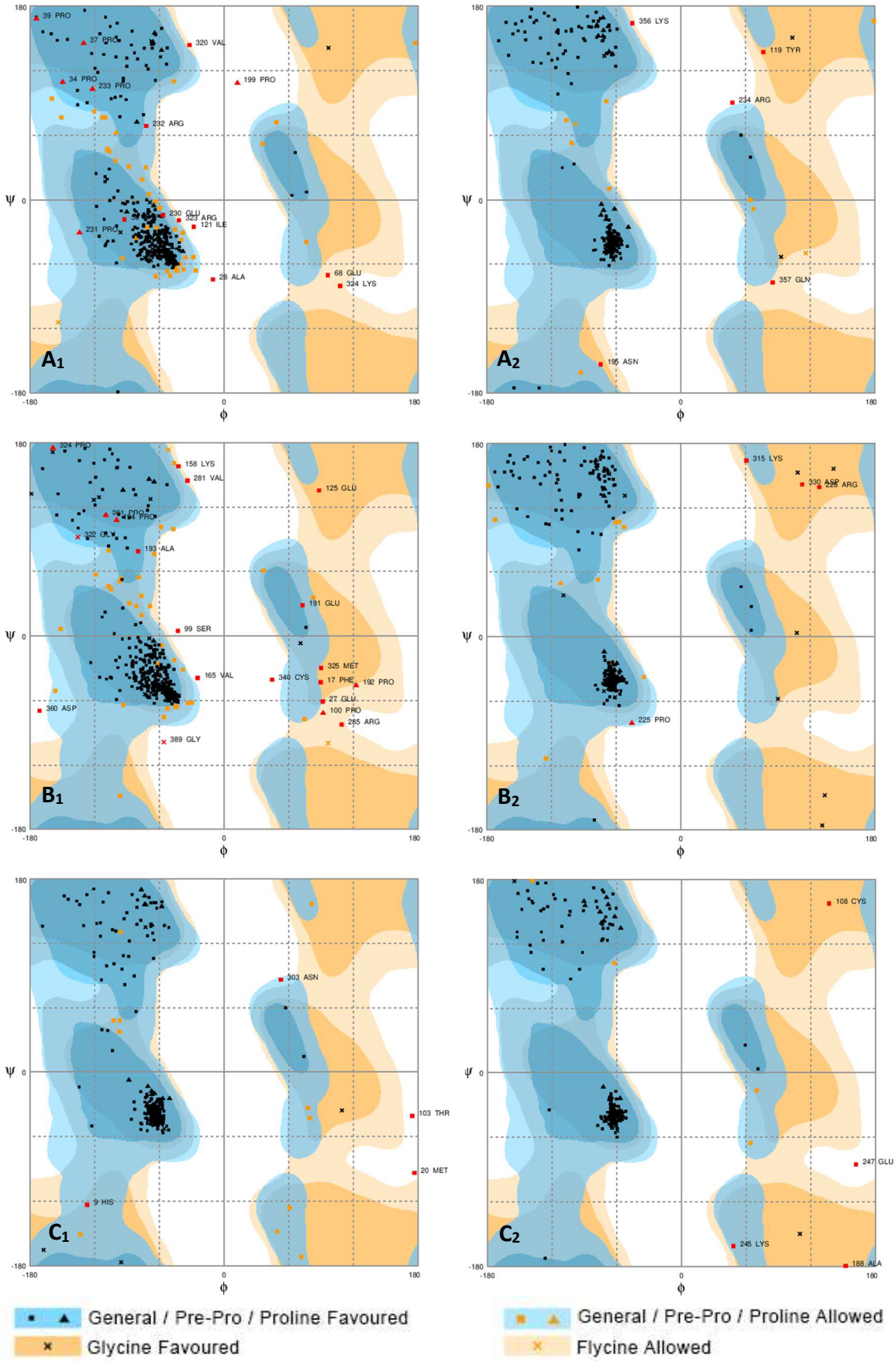

Fig. 11. Ramachandran plot generated with RAMPAGE of SSL-1 (A), SSL-2 (B), and SSL-3 (C) from *B. terribilis* AICB 870, before (subscript 1) and after (subscript 2) structure refinement. Red coloured amino acids are found in unallowed regions.

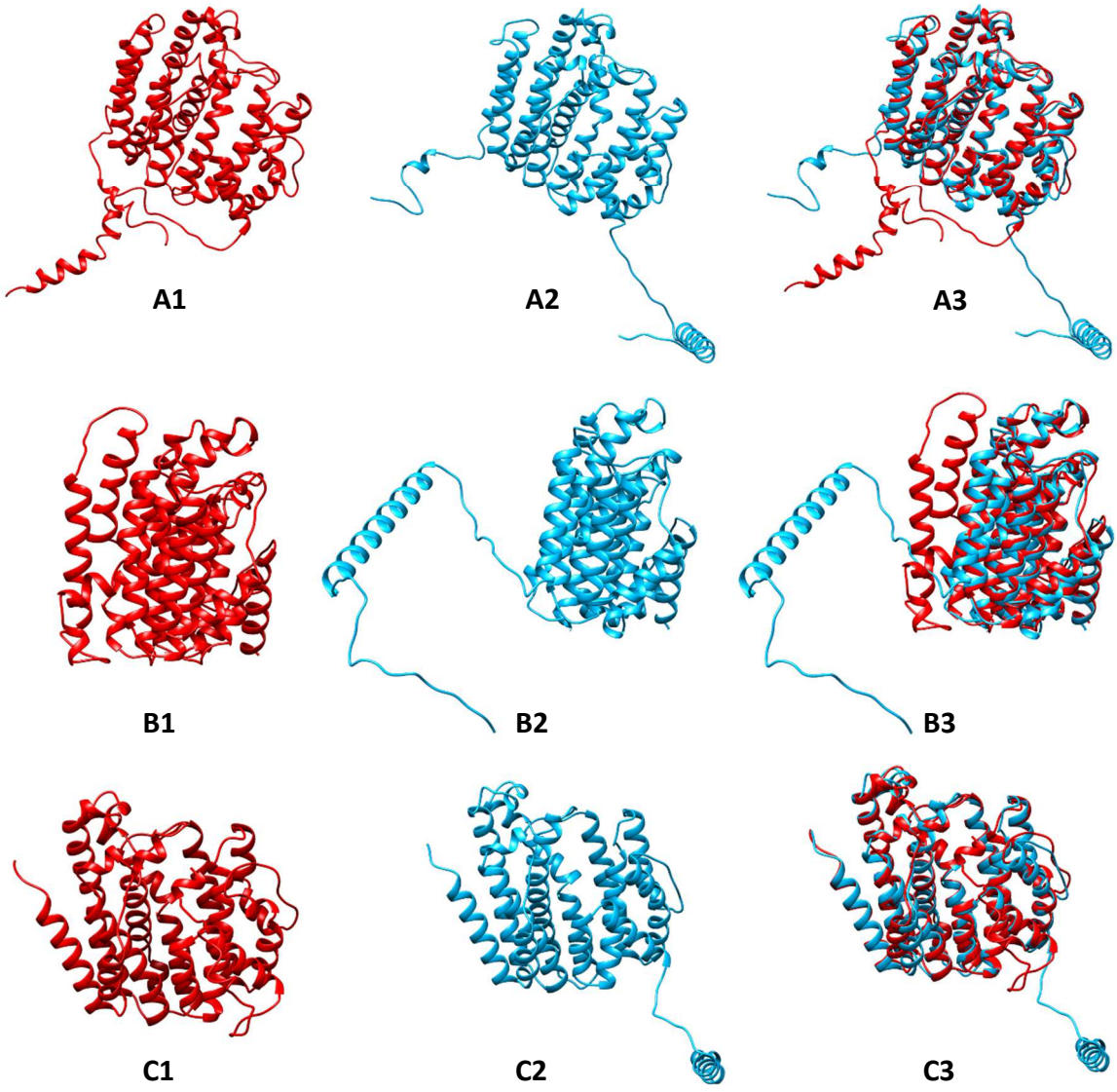

Fig. 12. Three-dimensional protein structures prediction of SSL-1 (A), SSL-2 (B) and SSL-3 (C) from *B. terribilis* AICB 870. 1 (red) – initial raw structure; before refinement, 2 (blue) – structure after refinement; 3 – superimposing of initial and final structure.

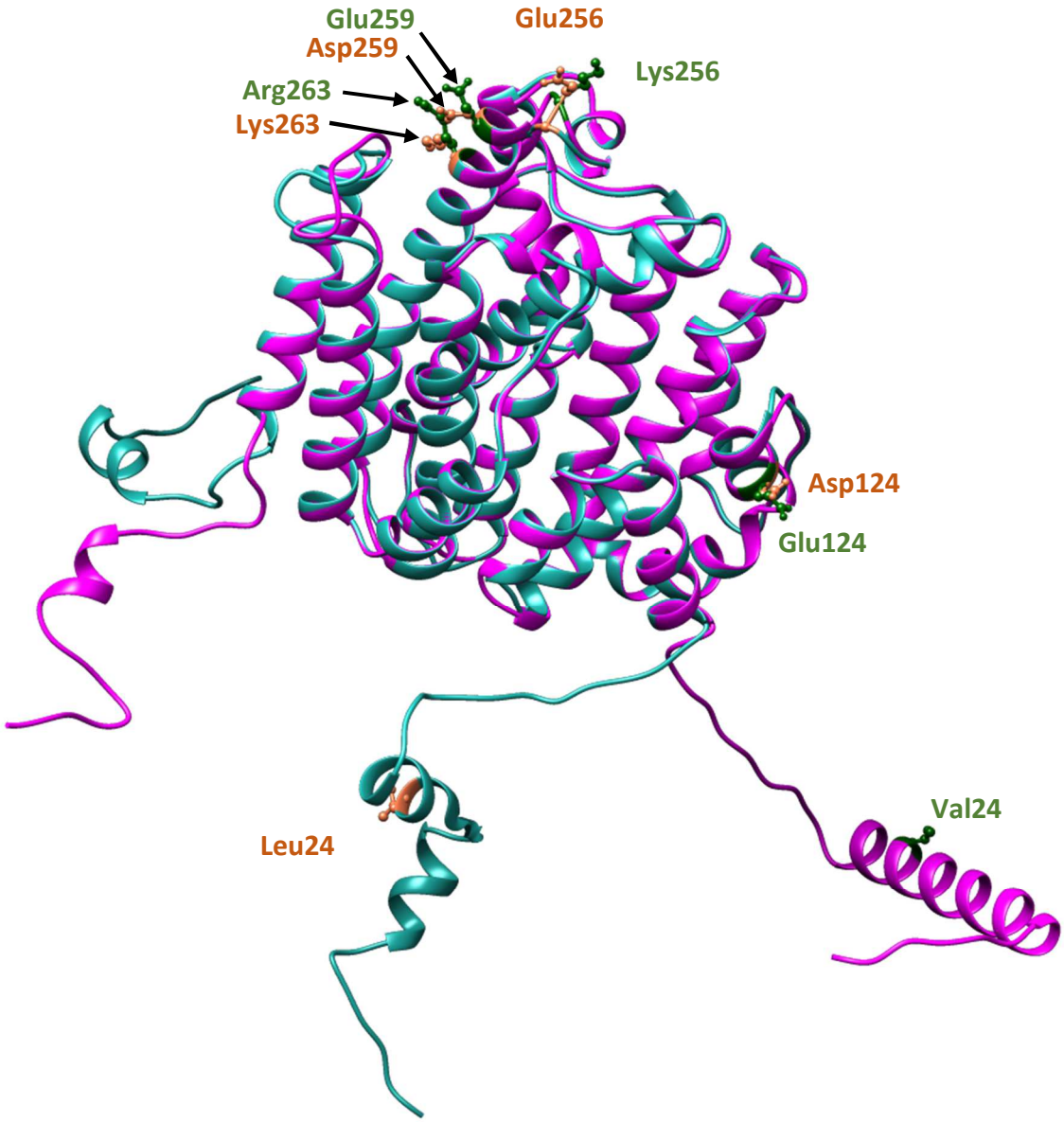

Fig. 13. Image illustrating the superimposed 3D - structures obtained after refinement of SSL-1 from *B. terribilis* AICB 870 (magenta) and *B. braunii* Showa (blue). The mismatched *aa* are indicated, in green (AICB 870) and orange (Showa).

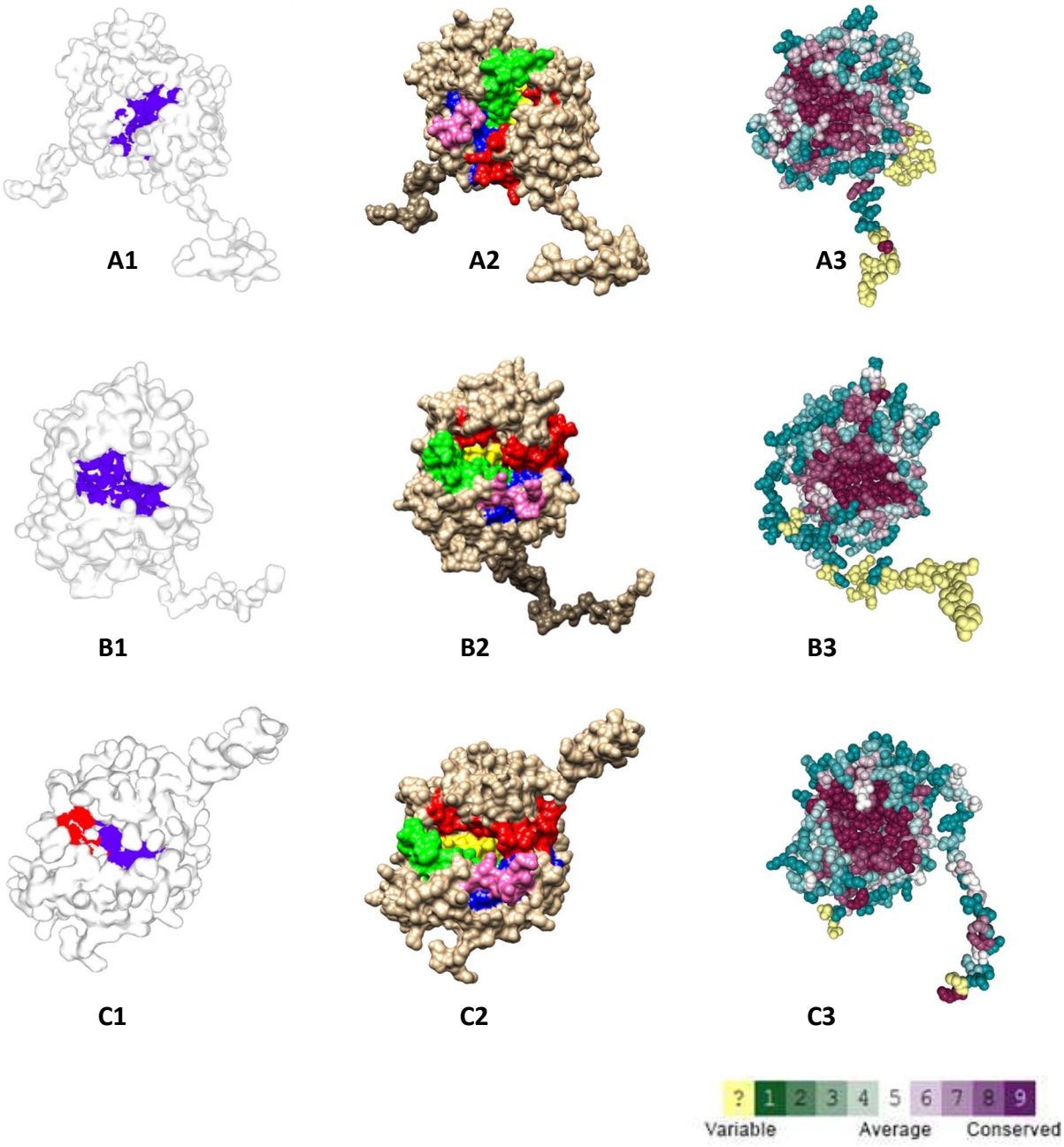

Fig. 14. (1) **-** Schematic representation of predicted pockets with P2Rank; (2) Representation of conserved domains according to Lee and Poulter (2008), Domain I – red, Domain II – yellow, Domain III – green, Domain IV – blue, NADPH - binding domain – pink; (3) – Conservation degree of *aa* residues according to ConSurf; from SSL-1 (A), SSL-2 (B) and SSL-3 (C) in *B. terribilis* AICB 870.

Squalene synthase-like are the enzymes involved in the biosynthesis pathway of hydrocarbons and were firstly described and characterized in the green microalga *Botryococcus braunii* (Niehaus *et al*., 2011). They described three enzymes generically named SSL-1 (EC: 2.5.1.103), SSL-2 (EC: 1.3.1.96) and SLL-3 (EC: 1.3.1.97), each enzyme being responsible for catalyzing one specific reaction in the synthesis pathway. The biosynthesis pathway of hydrocarbons in *B. braunii* and possibly, *B. terribilis*, starts from the head-to-head condensation of two FPP moieties to form a stable intermediate compound, PSPP. This reaction is catalyzed by SSL-1, afterwards, SLL-2 catalyze the NADPH-dependent conversion of PSPP to squalene. Similarly, botryococcenes biosynthesis occurs with a PSPP intermediate which is converted to botryococcenes by SSL-3 (Niehaus *et al.*, 2011).

The comparative analysis of before and after refinement of 3D protein structures highlighted the following: 1) the N-terminus of SSL-1 (AICB 870) was a disordered fragment formed by 14 amino acids which during refinement suffered a conformational change of 90° at Lys40 and Asp41, and at the C-terminus a similar conformation change occurred at Lys385; and 2) SSL-2 (AICB 870) showed the presence of an anchor which contains one of the transmembrane domains, the conformational change was due to the twist of Lys344 towards Ala343.

The 3D proteins structures were also analyzed for potential ligands and two ligands were discovered: FPS and PS7. Elumalai *et al*. (2018) observed that there is a third ligand, 8PH, in case of SQS from *B. braunii* BB1.

Squalene synthase from plants were overexpressed in medicinal plants such as *Panax ginseng* (Lee *et al.*, 2004) or *Eleutherococcus senticosus* (Seo *et al.*, 2005) in order to stimulate triterpenes or phytosterols production. Co-expression of both SSL-1 and SSL-3 from *B. braunii* Showa in yeasts yielded 100 mg L^{-1} botryococcenes synthesis (Niehaus *et al.*, 2011).

The number of papers which investigate the three-dimensional protein structure prediction and analysis of squalene synthase-like enzymes from *B. braunii* or other species belonging to *Botryococcus* is very low. From firstly being published in 2011 by Niehaus *et al*. Till now, only two other studies investigated the 3D protein structure of SSL in *B. braunii* Showa. These two studies are by Bell *et al*. (2014) and Elumalai *et al*. (2018). Bell *et al*. (2014) used 3D protein structure prediction and directed mutagenesis to understand the rearrangement of PSPP molecules at 1'-1 and 1'-3 bonds, and also tried to identify the amino acid residues and/or domains that were involved in this crucial step of the squalene and botryococcenes synthesis pathway.

GENERAL CONCLUSIONS

By studying the *B. terribilis* chemical race B algal strains deposited in the Algae and Cyanobacteria Collection of the Institute of Biological Research in Cluj-Napoca, this paper aimed at identifying the primary transcripts and the genes involved in squalene synthase activity by using a molecular approach and the three-dimensional protein structure prediction of squalene synthase-like based on *in silico* analysis.

- The molecular analysis lead to the identification of *de novo* designed primer pairs and establishing an amplification protocol for the primary transcripts and SSL genes which can lead to further investigations.

- Identification of the genes involved in squalene synthase activity appeared to be problematic due to their extended length (between 3800 and 6000bp) and the presence of repeated intronic regions, highly variable. Despite all these, the SSL-1 gene could be identified and analyzed in seven strains belonging to *B. terribilis*.

- The *in silico* analysis had two main purposes: establishing an experimental methodology for 3D protein structure prediction of SSL, quality assessment and refinement of predicted structures to generate three-dimensional models similar to the native ones; and a comparison between all obtained structures and the prediction of the conserved active sites involved in the last steps of squalene and botryococcene synthesis pathway.

- The methodology described for 3D protein structure prediction – analysis – refinement was very efficient, managing to significantly improve the quality of the predicted structures for SSL-1 and SSL-2 from *B. terribilis* AICB 870.

- The comparative analysis of the refined structures indicated minor modifications at the protein core, involved in FPP conversion to PSPP (SLL-1) and of PSPP to squalene (SSL-2) or botryococcene (SSL-3); the major changes were obtained where the loops and N and C-terminus regions are, but they were not important since these regions are not involved in the catalytic role of the protein. Studying the functional regions showed the presence of highly conserved pockets, two potential ligands (FPS and PS7), and Mg^{2+} divalent ions binding motifs, whose main purpose is to stabilize diphosphate groups found in the precursors used for hydrocarbon synthesis.

REFERENCES

Abraham, M. J., Murtola, T., Schulz, R., Páll, S., Smith, J. C., et al., 2015, GROMACS: High performance molecular simulations through multi-level parallelism from laptops to supercomputers, *SoftwareX*, **1-2**, pp. 19-25.

Achitouv, E., Metzger, P., Rager, M.N., Largeau, C., 2004, C_{31} - C_{34} methylated squalenes from a bolivian strain of *Botryococcus braunii*, *Phytochem.*, **65**, pp. 3159-3165.

Amit, M., Donyo, M., Hollander, D., Goren, A., Kim, E., et al., 2012, Differential GC content between exons and introns establishes distinct strategies of splice-site recognition, *Cell Rep.*, **1**, pp. 543-556.

Ashkenazy, H., Abadi, S., Martz, E., Chay, O., Mayrose, I., et al., 2016, ConSurf 2016: an improved methodology to estimate and visualize evolutionary conservation in macromolecules, *Nucleic Acids Res.*, **44**, pp. W344-W350.

Banerjee, A., Sharma, R., Chisti, Y., Banerjee, U. C., 2002, *Botryococcus braunii*: a renewable source of hydrocarbons and other chemicals, *Crit. Rev. Biotechnol.*, **22**, pp. 245-279.

Bell, S. A., Niehaus, T. D., Nybo, E., Chapell, J., 2014, Structure-function mapping of key determinants for hydrocarbon biosynthesis by squalene and squalene synthase-like enzymes from the green alga *Botryococcus braunii* race B, *Biochem.*, **53**, 7570-7581.

Bibi, R., Ahmad, Z., Imran, M., Hussain, S., Ditta, A., et al., 2017, Algal bioethanol production technology: A trend towards sustainable development, *Renew. Sust. Energ. Rev.*, **71**, pp. 976-985.

Blagg, B. S. J., Jarstfer, M. B., Rogers, D. H., Poulter, C. D., 2002, Recombinant squalene synthase. A mechanism for the rearrangement of presqualene diphosphate to squalene, *J. Am. Chem. Soc.,* **124**, pp. 8846-8853.

Brennan, L., Owende, P., 2010, Biofuels from microalgae – A review of technologies for production, processing, and extractions of biofuels and co-products, *Renew. Sust. Energ. Rev.,* **14**, pp. 557-577.

British Petroleum, 2019, BP Statistical Review of World Energy, 68th Edition.

Brown, A. C., Knights, B. A., Conway, E., 1969, Hydrocarbon content and its relationship to physiological state in green alga *Botryococcus braunii*, *Phytochem.*, **8**, 543-547.

Cantrell, K. B., Ducey, T., Ro, K. S., Hunt, P. G., 2008, Livestock waste-to-bioenergy generation opportunities, *Biores. Technol.*, **99**, pp. 7941-7953.

Chen, V. B., Arendall III, W. B., Headd, J. J., Keedy, D. A., Immormino, R. M., et al., 2009, MolProbity: all-atom structure validation for macromolecular crystallography, *Acta Cryst. D*, **66**, pp. 12-21.

Chisti, Y., 2007, Biodiesel from microalgae, *Biotechnol. Adv.*, **25**, pp. 294-306.

Choi, J. S., Kim, J. S., Joe, C. O., Kim S., Ha, K. S., et al., 1999, Improved cycle sequencing of GC-rich DNA template, *Exp. Mol. Med.*, **31**, pp. 20-24.

Consoletti, S. F., Prinsen, P., 2019, Carbon dioxide biosequestration and wastewater treatment using microalgae, in: Environmental Sustainability and Education for Waste Management. Education for Sustainability (Eds., So, W., Chow, C., Lee, J.), Springer, Singapore, pp. 241-270.

da Rosa, G. M., de Moris, M. G., Vieira Costa, J. A., 2018, Green alga cultivation with monoethanolamine: Evaluation of CO_2 fixation and macromolecule production, *Biores. Technol.*, **261**, pp. 206-212.

Dale, M., Krumdieck, S., Bodger, P., 2011, Net energy yield from the production of conventional oil, *Energy Policy*, **39**, 7095-7102.

Demirbas, A., 2016, Introduction, in: Waste Energy for Life Cycle Assessment, (Ed., Demirbas, A.,), Springer Internat. Publ., Switzerland, pp. 1-30.

Dismukes, G. C., Carrieri, D., Bennette, N., Ananyev, G. M., Posewitz, M. C., 2008, Aquatic phototrophs: efficient alternatives to land-based crops for biofuels, *Curr. Opin. Biotechnol.*, **19**, pp. 235-240.

Elumalai, S., Sangeetha, T., Rajesh Kanna,G., 2018, *In silico* modeling and characterization of squalene synthase and botryococcene synthase enzymes from a green photosynthetic microalga *Botryococcus braunii*, *J. Pet. Environ. Biotechnol.*, **9**, 3.

Gasteiger, E., Hoogland, C., Gattiker, A., Duvaud, S., Wilkins, M. R., et al., 2005, Protein Identification and Analysis Tools on the ExPASy Server, in: Proteomics Protocols Handbook, (Eds. Walker, J. M.), Humana Press, pp. 571-607.

Ghafari, M., Rashidi, B., Haznedaroglu, B. Z., 2018, Effects of macro and micronutrients on neutral lipid accumulation in oleaginous microalgae, *Biofuels*, **9**, pp. 147-156.

Ghawana, S., Paul, A., Kumar, H., Kumar, A., Singh, H., et al., 2011, An RNA isolation system for plant tissues rich in secondary metabolites, *BMC Research Notes,* **4**: 85.

Gu, P., Ishii, Y., Spencer, T. A:, Shechter, I., 1998, Function-structure studies and identification of three enzyme domain involved in the catalytic activity in rat hepatic squalene synthase, *J. Biol. Chem.*, **273**, pp. 12515-12525.

Hata, S., Sanmiya, K., Kouchi, H., Matsuoka, M., Yamamoto, N., Izui, K., 1997, cDNA cloning of squalene synthase genes from mono- adn dicotyledonus plant, and expression of the gene in rice, *Plant Cell Phisiol.*, **38**, pp. 1409-1413.

Hegedűs, A., Moca, A., Barbu-Tudoran, L., Coman, C., Dragoș, N., 2016, Molecular phylogeny of *Botryococcus braunii* strains (race A) – An integrative approach, *Algal Res.*, **19**, pp. 189-197.

Hegedűs, A., Mocan, A., Barbu-Tudoran, L., Coman, C., Drugă, B., Sicora, C., Dragoș, N., 2014, Morphological, biochemical, and phylogenetic assessments of eight *Botryococcus terribilis* strains collected from freshwaters of Transylvania, *J. Appl. Phycol.*, **27**, pp. 865-878.

Heo, L., Feig, M., 2018, PREFMD: a web server for protein structure refinement via molecular dynamics simulations, *Bioinformatics*, **36**, pp. 1063-1065.

Hirose, M., Mukaida, F., Okada, S., Noguchi, T., 2013, Active hydrocarbon biosynthesis and accumulation in a green alga *Botryococcus braunii* (Race A), *Eukaryot. Cell,* **12**, pp. 1132 - 1141.

Huang, Z., Poulter, C. D., 1989, Tetramethylsqualene, a triterpene from *Botryococcus braunii* var. Showa, *Phytochem.,* **28**, pp. 1467-1470.

Jendele, L., Krivák, R., Škoda, P., Novotný, M., Hoksza, D., 2019, PrankWeb: a web server for ligand binding site prediction and visualization, *Nucleic Acids Res.*, **47**, pp. W345-W349.

Judd, S. J., Al Momani, F. A. O., Znad, H., Al Ketife, A. M. D., 2017, The cost benefit of algal technology for combined CO_2 mitigation and nutrient abatement, *Renew. Sust. Energ. Rev.*, **71**, pp. 379-387.

Kawachi, M., Tanoi, T., Demura, M., Kaya, K., Watanabe, M. M., 2012, Relationship between hydrocarbons and molecular phylogeny of *Botryococcus braunii*, *Algal Res.*, **1**, pp. 114-119.

Kim, B. H., Ramanan, R., Cho, G. G., La, H. J., Ahn, C. Y., et al., 2012, Simple, rapid and cost-effective method for high quality nucleic acids extraction from different strains of *Botryococcus braunii*, *PLoS ONE*, **7**.

Kirtay, E., 2009, World's population and energy demand, *Soc. Polit. Econ. Cult. Res.*, **1**, pp. 145-169.

Komárek, J., Marvan, P., 1992, Morphological differences in natural populations of *Botryococcus* (Chlorophyceae), *Arch. Protistenkd*, **141**, pp. 65-100.

Krivák, R., Hoksza, D., 2018, P2Rank: machine learning based tool for rapid and accurate prediction of ligand binding sites from protein structure, *J. Cheminform.*, **10**, 39.

Kumar, S., Stecher, G., Tamura, K., 2016, MEGA7: Molecular Evolutionary Genetics Analysis version 7.0 for bigger datasets, *Mol. Biol. Evol.*, **33**, pp. 1870-1874.

Largeau, C., Casadevall, E., Berkaloff, C., 1980a, The biosynthesis of the long-chain hydrocarbon in the green alga *Botryococcus braunii*, *Phytochem.*, **19**, pp. 1081-1085.

Largeau, C., Casadevall, E., Berkaloff, C., Dhamelincourt, P., 1980b, Sites of accumulation and composition of hydrocarbons in *Botryococcus braunii*, *Phytochem.*, **19**, pp. 1043-1051.

Larkin, M. A., Blackshields, G., Brown, N. P., Chenna, R., McGettigan, P. A., et al., 2007, ClustalW and ClustalX version 2.0, *Bioinformatics*. **23**, pp. 2947-2948.

Lawrence, A. K., Mezulis, S., Yates, C. M., Wass, M. N., Sternberg, M. J. E., 2015, The Phyre2 web portal for protein modeling, prediction and analysis, *Nature Protoc.*, **10**, pp. 845-858.

Lee, S., Poulter, C.D., 2008, Cloning, solubilization, and characterization of squalene synthase from *Thermosynechococcus elongates* BP-1, *J. Bacteriol.*, **190**, pp. 3808 – 3816.

Lee, M. H., Jeong, J. H., Seo, J. W., Shin, C. G., Kim, Y. S., 2004, Enhanced triterpene and phytosterol biosynthesis in *Panax ginseng* overexpressing squalene synthase gene, *Plant Cell Physiol.*, **45**, pp. 976- 984.

Lovell, S. C., Davis, I. W., Arendall III, W. B., de Bakker, P. I. W., Word, J. M., et al., 2003, Structure validation by Calpha geometry: phi,psi and Cbeta deviation, *Prot. Struct. Funct. Genet.*, **50**, pp. 437-450.

Marzo, C., Díaz, A. B., Caro, I., Blandino, A., 2019, Status and perspectives in bioethanol production from sugar beet, in: Bioethanol Production from Food Crops, (Eds., Ramesh C. R., Ramachandran, S.), Acad. Press, pp. 61-79.

Mendes, M. C. Q., González, A. A. C., Moreno, M. L. V., Figueira, C. P., Nunes, J. M. C., 2012, Morphological and ultrastructure features of a strain of *Botryococcus terribilis* (Trebouxiophyceae) from Brazil, *J. Phycol.*, **48**, 1099-1106.

Metzger, P., Largeau, C., 2005, *Botryococcus braunii*: a rich source for hydrocarbons and related ether lipids, *Appl. Microbiol. Biot.,* **66**, pp. 486-496.

Metzger, P., Allard, B., Casadevall, E., Berkaloff, C., Coute, A., 1990, Structure and chemistry of a new chemical race of *Botryococcus braunii* that produces lycopadiene, a tetraterpenoid hydrocarbon, *J. Phycol.*, **26**, pp. 258-266.

Metzger, P., Casadevall, E., 1987, Lycopadiene, a tetraterpenoid hydrocarbon from new strains of the green alga *Botryococcus braunii*, *Tetrahedron Lett.*, **28**, pp. 3931-3934.

Metzger, P., Templier, J., Largeau, C., Casadevall, E., 1986, An *n*-alkatriene and some *n*-alkadienes from the A race of the green alga *Botryococcus braunii*, *Phytochem.*, **25**, pp. 1869-1872.

Metzger, P., Casadevall, E., Pouet, M.-J., Pouet, Y., 1985, Structures of some botryococcenes: branched hydrocarbons from the B race of the green alga *Botryococcus braunii*, *Phytochem.*, **24**, pp. 2995-3002.

Nakashima, T., Inoue, T., Oka, A., Nishino, T., Osumi, T., Hata, S., 1995, Cloning, expression, and characterization of cDNAs encoding *Arabidopsis thaliana* squalene synthase, *Proc. Natl. Acad. Sci. USA*, **92**, pp. 2328-2332.

Naik, S. N., Goud, V. V., Rout, P. K., Dalai, A. K., 2010, Production of first and second generation biofuels: A comprehensive review, *Renew. Sust. Energ. Rev.,* **14**, pp. 578-597.

Niehaus, T. D., Okada, S., Devarenne, T. P., Watt, D. S., Sviripa, V., Chappell, J., 2011, Identification of unique mechanisms for triterpene biosynthesis in *Botryococcus braunii*, *Proc. Natl. Acad. Sci. USA,* **108**, pp. 12260-12265.

Nigam, P. S., Singh, A., 2011, Production of liquid biofuels from renewable resources, *Progr. Energ. Combust.,* **37**, pp. 52-68.

Ortiz-Marquez, J. C. F., Do Nascimento, M., Zehr, J. P., Curatti, L., 2013, Genetic engineering of multispecies microbial cell factories as an alternative for bioenergy production, *Trends Biotechnol*., **31**, pp. 521-529.

Petersen, H. I., Rosenberg, P., Nytoft, H. P., 2008, Oxygen groups in coals and alginite-rich kerogen revisited, *Int. J. Coal. Geol.*, **74**, pp. 93-113.

Poulter, C. D., 1990, Biosynthesis of non-head-to-tail terpenes-formation of 1′-1 and 1′-3 linkages, *Acc. Chem. Res.*, **23**, pp. 70-77.

Ranga Rao, A., *Gogisetty, D., Gokare, R. A., Ravi, S., Bikkina, P. N., Su, Y., Lei, B., 2017, Botryococcus* as an alternative source of carotenoids and its possible applications – an overview, *Crit. Rev. Biotechnol.*, **38**, pp. 541-558.

Rodolfi, L., Zittelli, G. C., Bassi, N., Padovani, G., Biondi, N., Bonini, G., el al*.,* 2008, Microalgae for oil: strain selection, induction of lipid synthesis and outdoor mass cultivation in a low-cost photobioreactor, *Biotechnol. Bioeng.*, **102**, pp. 100-112.

Salama, E-S., Kurade, M. B., Abou-Shanab, R. A. I., El-Dalatony, M. M., Yang, Il-S., Min, B., Jeon, B.-H., 2017, Recent progress in microalgal biomass production coupled with wastewater treatment for biofuel generation, *Renew. Sust. Energ. Rev.*, **79**, pp. 1189-1211.

Searchinger, T., Heimlich, R., Houghton, R. A., Dong, F., Elobeid, A., Fabiosa, J., el al*.*, 2008, Use of U.S. croplands for biofuels increases greenhouse gases through emissions from land-use change, *Science*, **319**, pp. 1238-1240.

Seo, J. W., Jeong, J. H., Shin, C. G., Lo, S. C., Han, S. S., et al., 2005, Overexpression of squalene synthase in *Eleutherococcus senticosus* increases phytosterol and triterpene accumulation, *Phytochem.*, **66**, pp. 869-877.

Spolaore, P., Joannis-Cassan, C., Duran, E., Isambert, A., 2006, Commercial applications of microalgae, *J. Biosci. Bioeng.*, **101**, pp. 87- 96.

Thapa, H. R., Naik, M. T., Okada, D., Takada, K., Molnár, I., Xu. Y., Devarenne, T. P., 2016, A squalene synthase-like enzyme initiates production of tetraterpenoid hydrocarbons in *Botryococcus braunii* Race L, *Nature Commun.*, **7**, e11198.

Treviño, F. I., Sánchez-Castillo, P., Comas González, A., 2009, Contribution to the taxonomic study of the family Botryococcaceae (Trebouxiophyceae, Chlorophyta) in southern Spain, *Cryptogamie Algol.,* **30**, pp. 17-30.

Voloshin, R. A., Rodionova, M. V., Zharmukhamedov, S. K., Veziroglu, T. N., Allakhverdiev, S. I., 2016, Review: Biofuel production from plant and algal biomass, *Int. J. Hydrogen Energ.,* **41**, pp 17257-17273.

Wiederstein, M., Sippl, M. J., 2007, ProSA-web: interactive web service for the recognition of errors in three-dimensional structures of proteins, *Nucleic Acids Res*., **35**, pp. W407-W410.

Weiss, T. L., Roth, R., Goodson, C., Vitha, S., Black, I., et al., 2012, Colony organization in the green alga *Botryococcus braunii* (Race B) is specified by a complex extracellular matrix, *Eukaryot. Cell*, **11**, pp. 1424-1440.

Wolf, F. R., Cox, E. R., 1981, Ultrastructure of active and resting colonies of *Botryococcus braunii* (Chlorophyceae), *J. Phycol.,* **17**, pp. 395-405.

Yang, Z., Pei, H., Hou, Q., Jiang, L., Zhang, L., Nie, Z., 2019, Algal biofilm-assisted microbial fuel cell to enhance domestic wastewater treatment: Nutrient, organics removal and bioenergy production, *Chem. Eng. J.*, **332**, pp. 277-285.

Yang, J., Roy, A., Zhang, Y., 2013, Protein-ligand binding site recognition using complementary binding-specific substructure comparison and sequence profile alignment, *Bioinformatics*, **29**, pp.2588-2595.

SCIENTIFIC ACTIVITY

1. Published/accepted scientific papers

Szőke-Nagy, T., Porav, A. S., Dragos, N, *In silico* modelling and analysis of squalene synthase-like 1 (SSL-1) from green microalga *Botryococcus terribilis* AICB 872, *Studia UBB Biologia* – Acceped.

Szőke-Nagy, T., Hegedűs, A., Baricz, A., Chiriac, C., Szekeres E., Coman, C., Dragoș, N., 2015, Identification, isolation and bioinformatic analysis of squalene sinthase-like cDNA fragments in *Botryococcus terribilis* AICB 870 strain, *Studia UBB Biologia*, **LX** (1), pp. 23-37.

2. Scientific communications.

Szőke-Nagy, T., Baricz, A., Chiriac, C., Szekeres, E., Coman, C., Dragoș, N., 2015, Identification of gene encoding squalene synthase-like 1 in five *Botryococcus terribilis* AICB Strains, *7th National Congress with International Participation and 33th Annual Scientific Session of Romanian Society for Cell Biology*, Baia Mare, 10-14 June 2015, Bull. RSBC no. 43, pp. 50.

Szőke-Nagy, T., Hegedűs A., Coman, C., Drugă, B., Dragoș, N., 2014, Identification of Three Synthase-Like cDNA Fragments in Botryococcus terribilis AICB 870, a botryococcene producing microalga, *6th National Congress with International Participation and 32th Annual Scientific Session of Romanian Society for Cell Biology*, Târgu Mureș, 4-7 June 2014, Bull. RSBC no. 42, pp. 113.

Szőke-Nagy, T., Dragoș, N., 2012, 3D structure prediction of squalene-synthases from algae and plants, *16th Symposium of Biology Students in Europe*, Szeged-Gödöllő, 27 July - 6 August 2012, Hungary, pp. 48-49.

3. International/National conference and workshops.

12th International Conference on Halophilic Microorganisms, June 24-28, 2019, Cluj-Napoca, Romania – ORGANIZATOR.

11th International Conference on Processes in Isotopes and Molecules (PIM 2017), September 27-29, 2017, Cluj-Napoca, Romania.

7th Congress of European Microbiologists (FEMS 2017), July 9-13, 2017, Valencia, Spania.

6th International Conference on Environmental, Industrial and Applied Microbiology (BioMicroWorld 2015), October 28-30, 2015, Barcelona, Spain,

7th National Congress with International Participation and 33th Annual Scientific Session of Romanian Society for Cell Biology, June 10-14, 2015, Baia Mare, Romania.

Promotion and Dissemination in the field of Sustainable Development and Environmental Protection, December 11-14, 2014, Sinaia, România – Workshop.

6th National Congress with International Participation and 32th Annual Scientific Session of Romanian Society for Cell Biology, 4-7 June 2014, Târgu Mureș, Romania.

16th Symposium of Biology Students in Europe, Szeged-Gödöllő, July 27 - August 6, 2012, Hungary – Workshop.

4th International Congress and 30th Annual Scientific Session of Romanian Society for Cell Biology, June 13-17, 2012, Satu Mare-Debrecen, Romania-Hungary.

Electron microscopy in Romania, a new perspective of research in medicine and biology, June 6, 2012, București, România – Workshop.

4. Other research papers in ISI journals - first author.

Szőke-Nagy, T., Porav, A. S., Coman, C., Cozar, I. B., Dina, N. E., Tripon, C., 2018, Characterization of the action of antibiotics and essential oils against bacteria by surface-enhanced Raman spectroscopy and scanning electron microscopy, *Anal. Lett.*, https://doi.org/10.1080/00032719.2018.1430150, **52** (1), PIM Sp. Iss., pp. 190-200, (**IF 1.206**).

5. Other research papers in ISI journals – co-author.

Dragoș, N., Chiriac, C., Porav, S., **Szőke-Nagy, T.,** Coman, C., Török, L., Hegedűs, A., 2019, *Desmodesmus tropicus* (Chlorophyta) in the Danube Delta – reassessing the phylogeny of the series Maximi, *Eur. J. Phycol.*, https://doi.org/10.1080/09670262.2018.1558286 (**IF 2.481**).

Szekeres, E., Chiriac, C. M., Baricz, A., **Szőke-Nagy, T.,** Lung, I., Soran, M.-L., Rudi, K., Dragoș, N., Coman, C., 2018, Investigating antibiotics, antibiotic resistance genes, and microbial contaminants in groundwater in relation to the proximity of urban areas, *Environ. Pollut,* **236**, pp. 734-744 (**IF 4.358**).

Cozar, I. B., Colniță, A., **Szőke-Nagy, T.,** Gherman, A. M. R., Dina, N. E., 2017, Label-free detection of bacteria using surface-enhanced Raman scattering and principal component analysis, *Anal. Lett.*, https://doi.org/10.1080/00032719.2018.1445747, **52** (1), PIM Sp. Iss., pp. 177-189, (**IF 1.206**).

Dina, N. E., Zhou, H., Colniță, A., Leopold, N., **Szőke-Nagy, T.,** Coman, C., Haisch, C., 2017, Rapid single-cell detection and identification of pathogens by using surface-enhanced Raman spectroscopy, *Analyst*, **142**, pp. 1782-1789 (**IF 3.864**).

Dina, N. E., Colniță, A., **Szőke-Nagy, T.,** Porav, A. S., 2017, A critical review on ultrasensitive, spectroscopic-based methods for high-throughput monitoring of bacteria during infection treatment, *Crit. Rev. Anal. Chem.*, **47** (6) pp. 499-512 (**IF 3.231**).

Dina, N. E., Leș, A., Baricz, A., **Szőke-Nagy, T.,** Leopold, N., Sârbu, C., Banciu, H. L., 2017, Discrimination of haloarchaeal genera using Raman spectroscopy and robust methods for multivariate data analysis, *J. Raman Spectrosc.*, **48** (8), 2017, pp. 1122–1126 (**IF 2.879**).

Opriș, O., Soran, M. L., Lung, I., Trușcă, M. R. C., **Szőke-Nagy, T.,** Coman, C., 2016, The optimization of the antibiotics extraction from wastewaters and manure using Box–Behnken experimental design, *Int. J. Environ. Sci. Technol.,* **14** (3), pp. 473-480, DOI 10.1007/s13762-016-1165-2 (**IF 1.915**).

6. Research papers in other journals – co-author.

Chiriac, C. M., Barbu-Tudoran, L., Baricz, A., Szekeres, E., **Szőke-Nagy, T.,** Dragoș, N., Coman, C., 2015, Bacterial diversity in a microbial mat colonizing a man-made geothermal spring from Romania, *Studia UBB Biologia*, LX (1), pp. 2-22.

Szekeres, E., Dragoș, N., Porav, A. S., Baricz, A., Chiriac, C., **Szőke-Nagy, T.,** Coman, C., 2015, Evaluation of bio-resources: monitoring *Arthrospira* growth in supplemented brackish water, *Studia UBB Biologia*, LX, Sp. Iss., pp. 45-48.

Bica, A., Barbu-Tudoran, L., Drugă, B., Coman, C., Nicoară, A., **Szőke-Nagy, T.,** Dragoș, N., 2012, *Desmodesmus communis* (Chlorophyta) from Romanian freshwater: cenobial morphology and molecular taxonomy based on the ITS2 of new isolates, *Annals of the Romanian Society for Cell Biology*, XVII (1), pp. 16-28.

7. Patents.

Dina, N. E., Colniță, A., Marconi, D. S., **Szőke-Nagy, T.,** Gherman, A. M. R., Leopold, N., Ștefancu, A., 2018, Procedeu de detecție prin Spectroscopie Raman amplificată de suprafață (SERS) într-un sistem de curgere microfluidic utilizând un spot de argint ca substrat amplificator SERS –OSIM A00976/28.11.2018 application.

8. Book chapters.

Baricz, A., **Szőke-Nagy, T.,** Szekeres, E., Chiriac, C., 2016, Methods for nucleic acids extraction in: Methodological guide for monitoring antibiotics and antibiotic resistance in the

environment, (Ed. Coman, C.), ISBN 978-606-561-165-8, Publisher Accent, Cluj-Napoca, Romania, pp. 41-62.

Hegedűs, A., **Szőke-Nagy, T.,** Butiuc-Keul, A., 2016, Identification of Antibiotic Resistant Microorganisms and the Antibiotic Resistance Genes, in: Methodological guide for monitoring antibiotics and antibiotic resistance in the environment, (Ed. Coman, C.), ISBN 978-606-561-165-8, Publisher Accent, Cluj-Napoca, Romania, pp. 227-306.

9. Other Scientific communications

Colniță, A., **Szőke-Nagy, T.,** Gherman, A.-M. R., Cozar, I. B., Dina, N. E., 2018, Detection and identification of pathogenic microorganisms using ultrasensitive Raman spectroscopy, *Conferința Națională de Biofizică*, September 7, București, Romania – *Oral presentation.*

Colniță, A., Gherman, A. M. R., **Szőke-Nagy, T.,** Cozar, I. B., Dina, N. E., 2018, The use of *in situ* surface enhanced Raman spectroscopy technique for antibiotic resistance determination of pathogenic microorganisms, *International Conference on Analytical and Nanoanalytical Methods for Biomedical and Environmental Sciences* (IC-AMBES 2018), May 23-25, Brașov, Romania – POSTER.

Buimaga-Iarinca, L., Morari, C., Colniță, A., Neamțu, S., Fischer-Fodor, E., **Szőke-Nagy, T.,** Farcas, A., Turcu, I., 2018, IMAGCELL – Assessing living cells natural features by employing optical microscopy and statistical analysis, *International Conference on Analytical and Nanoanalytical Methods for Biomedical and Environmental Sciences* (IC-AMBES 2018), May 23-25, Brașov, Romania – *Oral presentation.*

Gherman, A. M. R., Marconi, D., Colniță, A., Szabo, L., Leopold, N., **Szőke-Nagy, T.,** Dina, N. E., 2018, Microfluidic portable device for pathogens' rapid SERS detection, *International Conference on Analytical and Nanoanalytical Methods for Biomedical and Environmental Sciences* (IC-AMBES 2018), May 23-25, Brașov, Romania – POSTER.

Porav, S., **Szőke-Nagy, T.,** Dina, N. E., Cozar, B., Muntean, C., Tripon, C., 2017, Structural features induced in pathogenic bacteria by their interaction with natural and synthetic antibiotic agents, *11th International Conference on Processes in Isotopes and Molecules* (PIM 2017), September 27-29, Cluj-Napoca, România Spania – POSTER.

Szőke-Nagy, T., Gherman, A. M. R., Colniță, A., Cozar, I. B., Dina, N. E., 2017, Antibiotic susceptibility of *Aeromonas hydrophilia* monitored through SERS mapping methodology, *11th International Conference on Processes in Isotopes and Molecules* (PIM 2017), September 27-29, Cluj-Napoca, România Spania – POSTER.

Hegedus, A., Porav, S., **Szőke-Nagy, T.,** Torok, L., Coman, C., Dragoș, N., 2017, *Desmodesmus tropicus* in Danube Delta: morphological and phylogenetic approaches, *1st International*

Congrtess of Danube Region Botanical Gardens, September 7-9, Arad, Romania – POSTER.

Dina, N. E., Colniţă, A., Cozar, I. B., **Szőke-Nagy, T.,** 2017, Bacterial barcoding - a SERS mapping technique for ultrasensitive detection of pathogens*, 3rd International Conference on Enhanced Spectroscopies* (ICES 2017), Septembrie 4-7, München, Germania – POSTER.

Szőke-Nagy, T., Dina, N. E., Colniță, A., Cozar, I. B., 2017, Bacterial cell membrane barcoding, a SERS mapping methodology for identificaton and detection of potential pathogenic bacteria, *7th Congress of European Microbiologists* (FEMS 2017), July 9-13, Valencia, Spania – POSTER.

Szőke-Nagy, T., Dina, N. E., Porav, S., Tripon, C., 2017, Antimicrobial and inhibitory effects of therapeutic-grade essential oils against three environmental isolated bacterial strains, *7th Congress of European Microbiologists* (FEMS 2017), July 9-13, Valencia, Spania – POSTER.

Szekeres, E., Barcz, A. I., Chiriac, C. M., **Szőke-Nagy, T.,** Andrei, Ș. A., Coman C., 2016, Antibiotics and antibiotic resistant microorganisms: anthropic impact on natural environments, "*Kolozsvári Biológus Napok*", April 2016*,* Cluj-Napoca, Romania – *Oral presentation.*

Szekeres, E., Dragoș, N., Porav, A. S., Baricz, A., Chiriac, C., **Szőke-Nagy, T.,** Coman, C., 2015, Evaluation of Bio-Resources: Monitorig *Arthospira* growth in supplemented rackish water, *International Conference: Molecular Biology – Current Aspects and Prospects*, Novembre 6-8, Cluj-Napoca, Romania, – POSTER.

Andrei, Ș. A., Szekeres, E. K., **Szőke-Nagy, T.,** Chiriac, C. M., Baricz, A. I., Dragoș, N., Coman, C., 2015, Environmental filtering reduces antibiotic resistance genes abundance in urban wastewater treatment plants, *6th International Conference on Environmental, Industrial and Applied Microbiology* (BioMicroWorld 2015), Octobre 28-30, Barcelona, Spain – POSTER.

Chiriac, CM., Szekeres, E. K., Baricz, A. I., **Szőke-Nagy, T.,** Andrei, Ș. A., Dragoș, N., Coman, C., 2015, Evaluation of antibiotic resistance genes in human impacted environments from Romania: a preliminary step for an environmental protection strategy, *6th International Conference on Environmental, Industrial and Applied Microbiology* (BioMicroWorld 2015), Octobre 28-30, Barcelona, Spain – POSTER.

Coman, C., Baricz, A. I., Chiriac, C. M., Szekeres, E. K., **Szőke-Nagy, T.,** Andrei, Ș. A., Dragoș, N., 2015, A methodological framework to monitor pollution with antibiotics and antibiotic resistant microorganisms – the EnviroAMR project, *6th Internationa Conference on Environmental, Industrial and Applied Microbiology* (BioMicroWorld 2015), Octobre 28-30, Barcelona, Spain – POSTER.

Chiriac, C., Baricz, A., Szekeres, E., **Szőke-Nagy, T.,** Dragoș, N., Coman, C., 2015, A perspective on the ecological functions of antibiotics in natural environments, *7th National Congress with International Participation and 33th Annual Scientific Session of Romanian Society for Cell Biology*, June 10-14, Baia Mare, Romania, Bull. RSBC no. 43, pp. 36 – POSTER.

Hegedűs (Bica), A., Coman, C., Drugă, B., **Szőke-Nagy, T.,** Sicora, C., Dragoș, N., 2013, Single-colony PCR, a new molecular technique in studying the *Botryococcus* Genus Diversity, *Deltas and Wetlands*, nr. 1, Tulcea, pp. 13 – POSTER.

Filip, A., Uţiu, I., Munteanu, C., Guțu, M., **Szőke-Nagy, T.,** Crăciun, C., Guţu, D., Lang, C., Roşioru, C., 2012, *Trigonella foenum-graecum* seeds - a natural hepatoptotector, *4rd International Congress* and *30th Annual Scientific Session of Romanian Society for Cell Biology*, June 13-17, Satu Mare-Debrecen, Bull. RSBC no. 40, p. 59 – POSTER.

Szőke-Nagy, T., Pribac, G., Tripon, S., Crăciun, C., Roșioru C., 2012, Ultrastructural modifications in the liver of streptoyotocin-induced diabetic rats *4rd International Congress and 30th Annual Scientific Session of Romanian Society for Cell Biology*, June 13-17, Satu Mare-Debrecen, – *Oral presentation.*

Trif, M., Filip, A., Crăciun, C., Munteanu, C., Uţiu, I., **Szőke-Nagy, T.,** Lukaci, C., Tripon, S., Roşioru, C., 2012, Biologica activities of furil-benzothiazole (R)- and (S)- enantiomers and racemic in the liver of ethanol-intoxicated rats, *4rd International Congress* and *30th Annual Scientific Session of Romanian Society for Cell Biology*, June 13-17, Satu Mare-Debrecen,, Bull. RSBC nr. 40, p. 57 – POSTER.

10. Research project team member.

- PN-III-P1-1.2-PCCDI-2017-0010: „Emerging molecular technologies based on micro and nano-structured systems with biomedical applications".
- PN-III-P1-1.2-PCCDI-2017-0387: "Emerging technologies for the industrial capitalization of 2d structures (graphene and nongraphenic)".
- PN-III-P1-1.1-TE-2016-0032: "Design of highly efficient antimicrobial peptides: in silico prediction and experimental validation".
- PN-III-P2-2.1-PED-2016-0983: „Development of a microfluidic portable device for pathogen's rapid SERS detection".
- Granturi EEA 2009-2014 - 3499/20.05.2015: "Methodological guide for monitoring antibiotic residues and antimicrobial resistance in the environment as a supporting instrument for an enhanced quality management of surface waters and groundwater (EnviroAMR)".
- PN-II-RU-TE-2014-4-0862: "Pathogenic microorganisms' rapid detection and identification using high sensitive raman spectroscopy".